Acta Pharmaceutica Sinica B 2024;14(5):1987–2005

Chinese Pharmaceutical Association
Institute of Materia Medica, Chinese Academy of Medical Sciences

Acta Pharmaceutica Sinica B

www.elsevier.com/locate/apsb
www.sciencedirect.com

REVIEW

Discovery of GluN2A subtype-selective *N*-methyl-D-aspartate (NMDA) receptor ligands

Liyang Jiang[†], Na Liu[†], Fabao Zhao, Boshi Huang, Dongwei Kang, Peng Zhan[*], Xinyong Liu[*]

Department of Medicinal Chemistry, Key Laboratory of Chemical Biology (Ministry of Education), School of Pharmaceutical Sciences, Cheeloo College of Medicine, Shandong University, Jinan 250012, China

Received 21 September 2023; received in revised form 4 December 2023; accepted 28 December 2023

KEY WORDS

NMDA receptors;
GluN2A subtype;
Subtype-selective ligands;
SARs;
Protein ligand interactions

Abstract The *N*-methyl-D-aspartate (NMDA) receptors, which belong to the ionotropic Glutamate receptors, constitute a family of ligand-gated ion channels. Within the various subtypes of NMDA receptors, the GluN1/2A subtype plays a significant role in central nervous system (CNS) disorders. The present article aims to provide a comprehensive review of ligands targeting GluN2A-containing NMDA receptors, encompassing negative allosteric modulators (NAMs), positive allosteric modulators (PAMs) and competitive antagonists. Moreover, the ligands' structure–activity relationships (SARs) and the binding models of representative ligands are also discussed, providing valuable insights for the clinical rational design of effective drugs targeting CNS diseases.

*Corresponding authors.
E-mail addresses: zhanpeng1982@sdu.edu.cn (Peng Zhan), xinyongl@sdu.edu.cn (Xinyong Liu).
[†]These authors made equal contributions to this work.
Peer review under the responsibility of Chinese Pharmaceutical Association and Institute of Materia Medica, Chinese Academy of Medical Sciences.

https://doi.org/10.1016/j.apsb.2024.01.004

1. Introduction

L-Glutamate (L-Glu), which serves as the primary excitatory neurotransmitter in the central nervous system (CNS), plays a pivotal role in various brain functions. Disruptions in glutamatergic neurotransmission contribute to the pathogenesis of psychiatric disorders[1−4]. The glutamate receptors can be primarily classified into two groups, ionotropic Glu receptors (iGluRs) and metabotropic Glu receptors (mGluRs)[4−8]. mGluRs belong to G protein-coupled receptor (GPCR) superfamily, which regulate intracellular second messengers production through G-protein coupling and induce metabolic alterations[9,10]. The iGluRs regulate the majority of excitatory signaling in CNS[11−14], which can be further classified into three major families: *N*-methyl-D-aspartate (NMDA) receptors, α-amino-3-hydroxy-5-methyl-4-isoxazole-propionic acid (AMPA) receptors and kainate (KA) receptors[15,16]. NMDA receptors have captivated neuroscientists and pharmacologists since their discovery due to their prominent roles in synaptic plasticity as well as various neurological and psychiatric disorders such as pain, stroke, epilepsy, schizophrenia, post-traumatic stress disorder, depression, and neurodegenerative disease[17−21]. Therefore, NMDA receptors hold great promise as targets for studying a multitude of neurological diseases and for drug development.

NMDA receptor channels have a unique gating mode, which is both ligand-gated and voltage-gated, and has voltage-dependent Mg^{2+} blocking effect. When NMDA receptor is excited, it is not only permeable to univalent ions Na^{+} and K^{+}, but also highly permeable to Ca^{2+}. NMDA receptor parameters are involved in many complex biological and pathological mechanisms. GluN2A is a regulatory subunit of NMDA receptors and is not expressed when it exists independently. Its insertion modifies the function properties of the whole receptor and enhances the reaction to excitatory amino acids (EAA)[22−25].

NMDA receptors are heterotetramers composed of four subunits[22−32] (Fig. 1), including two required GluN1 subunits and two variable GluN2 subunits (2A−2D) or GluN3 subunits (3A, 3B). The GluN1 and GluN3 subunits bind glycine (Gly) or D-serine (D-Ser), while the GluN2 subunit binds Glu[33−37]. Regardless of the composition of the subunits, each subunit of NMDA receptors can be divided into four domains (Fig. 1): Extracellular N-terminal domain (NTD), which is primarily involved in subunit assembly and regulation; Agonist binding domain (ABD), where endogenous agonists interact; Transmembrane domain (TMD), the region housing then ion channel, consisting of three transmembrane helices and a hairpin loop; Intracellular C-terminal domain (CTD), mainly involved in receptor transport, anchoring and interaction with other intracellular molecules[38−45].

The functional properties of different subtypes of NMDA receptors primarily rely on the expression of various GluN2 subunits. Distinct expression patterns of the four GluN2 subunits are observed in specific brain regions and cell types, leading to variations in their connection with multiple neurophysiological and neuropathological processes as well as their correlation with diverse diseases[46−49]. GluN2A exhibits high expression levels in the hippocampus and cerebral cortex, while displaying moderate expression in the midbrain, cerebellum, striatum and brainstem. These brain areas are closely associated with depression, epilepsy, cerebral ischemia, schizophrenia, etc.[50−61]. GluN2B is predominantly distributed in hippocampus, cortex and striatum. It has emerged as a therapeutic target for ischemic stroke, schizophrenia and neuropathic pain[39,62−65]. GluN2C is mainly expressed in the cerebellum and thalamus whereas GluN2D is primarily localized in the brainstem and forebrain. Recent reports indicate that GluN2C or GluN2D subunit involvement can be observed in cognitive function impairment, sensory motor gating deficits, cortical excitation-inhibition imbalance, and thalamocortical rhythm abnormalities along with neuronal maturation disturbances[66−76]. From a pathological perspective, Parkinson's disease, social cognitive impairment, ischemic stroke developmental, epileptic encephalopathy and levodopa-induced motor disorders have been linked to these two subunits[77−81].

In this paper, our focus will be on the research findings of the effective and selective GluN2A negative allosteric modulators (NAMs), positive allosteric modulators (PAMs) and antagonists that have been identified in recent years. Additionally, we will review the progress made in studying these structures, their structure−activity relationships (SARs) and binding models of representative ligands to pave the way for further development of GluN2A subtype selective molecules.

2. Selective GluN2A-containing NMDA receptors NAMs

2.1. *Benzenesulfonamide analogues*

In a high-throughput screening, Bettini et al. identified a series of sulfonamide derivatives, exemplified by derivative **1**, TCN-201 (IC_{50} = 109 nmol/L) and **2** (IC_{50} = 3.98 μmol/L), as well as thiodiazole derivative **3** (IC_{50} = 3.8 μmol/L), which were novel NMDA receptor ligands (Fig. 2). These compounds were the first selective antagonists at GluN1/2A over GluN1/2B in 2010[82]. The inhibitory activity of TCN-201 was disrupted by high concentration of Gly and its mode of action resembled that of a competitive antagonist; however, further analysis revealed that it acted as NAMs and could reduce the affinity of Gly and D-Ser[83,84]. These compounds serve as valuable tools for investigating the specific role played by the GluN2A subunit under both physiological and pathological conditions.

The X-ray co-crystal structure of TCN-201 with GluN1/2A ABD (PDB code: 5I56) demonstrated that the binding site of TCN-201 is located at the interface between the ABDs of the GluN1 and GluN2A subunits, resulting in a conformational change of the receptor and ultimately preventing Gly from binding to the orthosteric binding site on GluN1 subunit. Additionally, as shown in Fig. 3, TCN-201 exhibited an unconventional binding conformation characterized by a U-shaped or hairpin-like $\pi-\pi$ stacking motif formed by its two benzene rings. The halogenated aromatic A ring of TCN-201 formed a sandwich structure with the aromatic benzene ring in its middle (B ring), leading to a parallel orientation stabilized by $\pi-\pi$ interactions. The results indicated that Gly binding stabilizes the closed conformation of GluN1 ABD, promoting contact between GluN2A Val783 and GluN1 Phe754, which results in low-affinity NAM binding. Conversely, when bound to glycine-cleavage sites, an open conformation of GluN1 ABD disrupts contact between GluN2A Val783 and GluN1 Phe754, leading to high-affinity NAM binding. This inhibition mechanism and selectivity are attributed to Val783 in the GluN2A subunit and Phe754 in the GluN1 subunit[83,84]. According to computer modeling studies depicted in Fig. 3, Arg755 and Tyr535 residues within the GluN1 subunit participate in cation$-\pi$ and $\pi-\pi$ interactions during ligand binding (Fig. 3).

As TCN-201 was discovered through high-throughput screening, systematic SARs were not initially reported. Furthermore, its applicability in biological studies proved challenging due

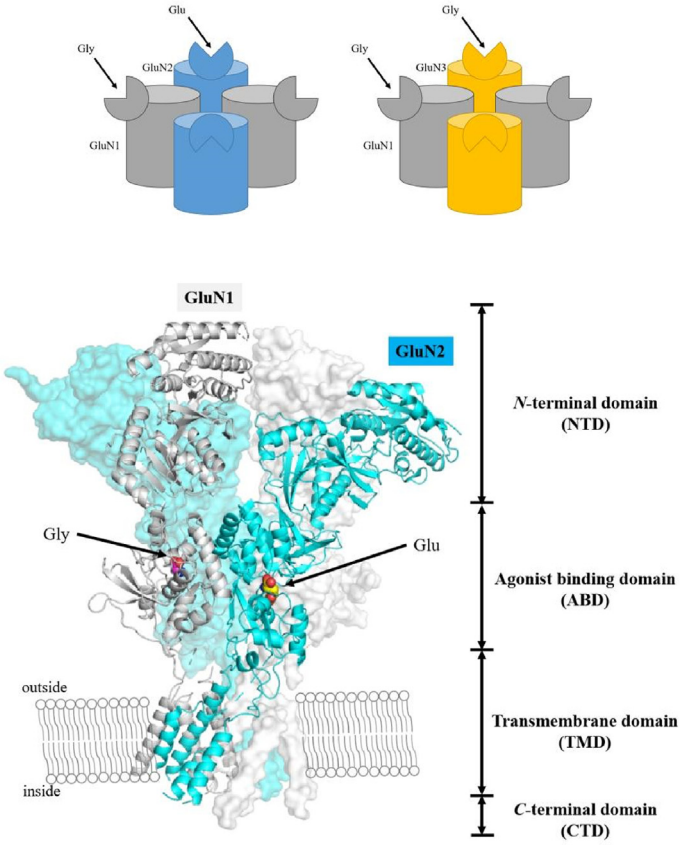

Figure 1 The architecture of NMDA receptors (PDB code: 4PE5). Color code: GluN1, grey; GluN2, blue; GluN3, orange[36].

low solubility. Therefore, the Bernhard group conducted various modifications based on TCN-201 to develop novel NAMs for GluN2A subunit-containing NMDA receptors with high activity[85]. The systematic variations included modifications to the halogen substituted phenyl ring A, middle phenyl ring B, right phenyl ring C and dihydrazide part (Fig. 4).

2.1.1. *Modifications on phenyl ring A*

The SARs (Fig. 5) demonstrated that substitutions of phenyl ring A at the *ortho*- or *para*-position resulted in a loss of activity, while motifs at the *meta*-position showed potential for enhancing GluN1/2A inhibition activity. Introducing a single halogen atom (-Cl, -Br or -I) at the *meta*-position generally led to a significant increase in potency of the analogue. Among them, analogue **4** with 3-bromobenzenesulfonamide (Inorm = 1.273) exhibited remarkable enhancement in inhibitory efficacy by achieving 127.3% compared to TCN-201 (Inorm = 1). However, replacing of the *meta*-halogen atom by methyl, nitro, methoxy or cyano moieties resulted in decreased activity. Furthermore, the high GluN1/2A activity observed for analogue **5** with 3-chlorobenzenesulfonamide (Inorm = 1.214) indicated that the presence of 4-fluoro atom of TCN-201 was not essential for obtaining high GluN1/2A inhibition among analogues. These findings suggest distinct properties associated with different halogen atoms as supported by *in silico* studies and imply that halogen atoms, particularly bromine substituent, may form halogen bonds with receptors and enhance the ligand binding affinity[85].

Replacement of the phenyl ring A with electron-deficient heterocycles resulted in a significant reduction in channel inhibition, as observed with 2-pyridiyl analogue **6** (Inorm = 0.151). Conversely, the introduction of an electron-rich ring, such as the 2-thienyl analogue **7** (Inorm = 0.529), enhanced antagonistic activity. Analogues substituted with heteroaryl, alkyl and allylic residues exhibited similar profiles. However, all benzene ring substitution analogues demonstrated weaker activities compared to TCN-201.

2.1.2. *Modifications on phenyl ring B*

As previously mentioned, TCN-201 displayed a U-shaped binding conformation, which resulted from the intermolecular $\pi-\pi$

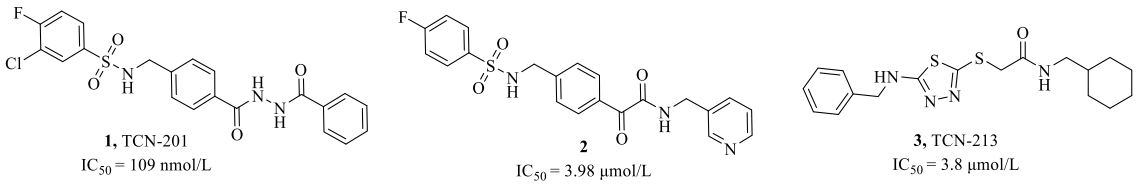

Figure 2 Chemical structure of representative compounds as GluN1/2A NAMs.

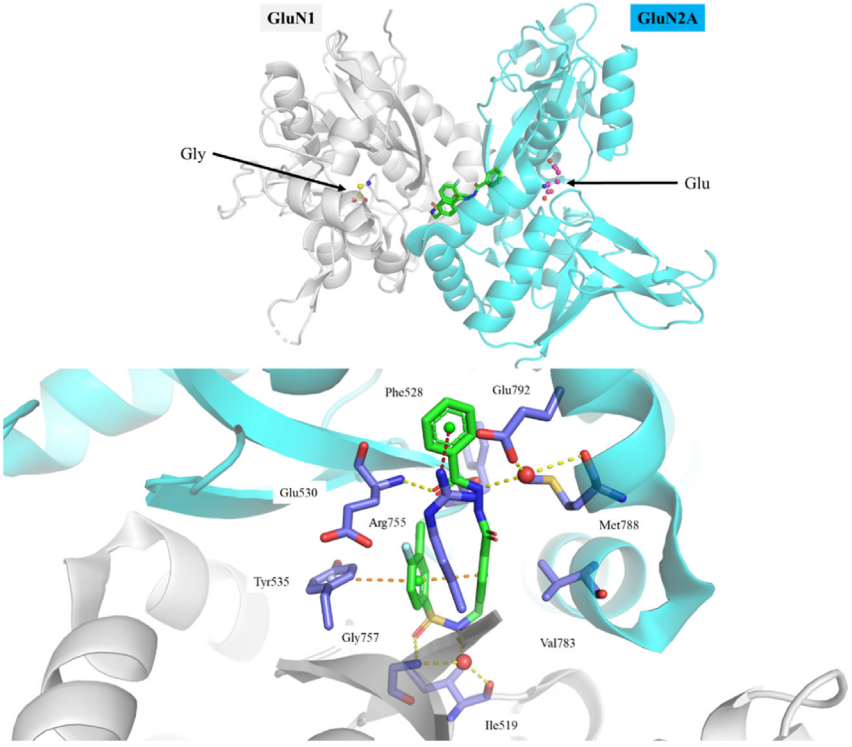

Figure 3 Binding mode of TCN-201 (GluN1: white cartoon; GluN2A: cyan cartoon; TCN-201: green stick; representative residues: blue stick; hydrogen bond: yellow dashed line; $\pi-\pi$ stacking: orange dashed line; cation$-\pi$ stacking: red dashed line. PDB code: 5I56)[83].

stacking of benzene rings A and B (Fig. 3)[86]. To enhance the accumulation with ring A and the interaction with surrounding residues, various electron-rich five-membered heterocyclic rings (thiazoles, oxazoles, isoxazoles, etc., Fig. 6) were substituted for the electron-deficient phenyl ring B. Regrettably, all compounds exhibited diminished activity compared to TCN-201, indicating that the benzene ring played a crucial role in maintaining potency.

2.1.3. *Modifications on phenyl rings A and B*

In order to enhance the $\pi-\pi$ interactions between the aromatic rings, thereby aligning them in a parallel manner, the substitution of aromatic rings A and B of TCN-201 was accomplished by a [2.2] paracyclophane system (Fig. 7). Three different types of TCN-201 analogues based on [2.2]paracyclophane-based were designed to validate the unique U-shaped conformation of NAMs within the binding pocket of GluN1/2A NMDA receptors[87,88]. Although docking studies demonstrated that the conformationally constrained [2.2]paracyclophane system was tolerated by the NMDA receptor, none of these analogues exhibited desirable inhibitory potencies. The most potent analogue **8** (Inorm = 0.36) in this series only achieved 36% inhibitory efficacy compared to TCN-201 (Inorm = 1). Neither compound **9** (Inorm = 0.02) or compound **10** (Inorm = 0.01) displayed significant inhibitory activity. Consequently, it can be speculated that TCN-201 is able to easily access the binding pocket due to its flexible connection between its aromatic components, resulting in superior inhibitory activity.

2.1.4. *Modifications on phenyl ring C*

Unlike the dominant effects of phenyl ring B, substitution of phenyl ring C with different groups led to analogues exhibiting diverse potency profiles (Fig. 8)[89]. When electron-rich five-membered heterocyclic rings were used as replacements for phenyl ring C, generally improved potencies compared to TCN-201 could be achieved. Specifically, moderate potency enhancement was observed for furan and pyrrole derivatives, while thiophene derivative **11** (Inorm = 1.35) displayed significantly superior activity than TCN-201. The SARs suggested that inhibitory activity was correlated to the aromaticity of five-membered rings; furan-substituted analogues with lower aromaticity

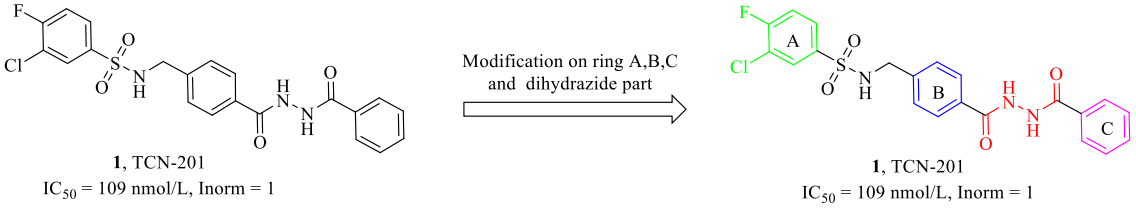

1, TCN-201
IC_{50} = 109 nmol/L, Inorm = 1

1, TCN-201
IC_{50} = 109 nmol/L, Inorm = 1

Figure 4 Modifications of TCN-201, Inorm (the normalization of the inhibition was related to the inhibition of TCN-201).

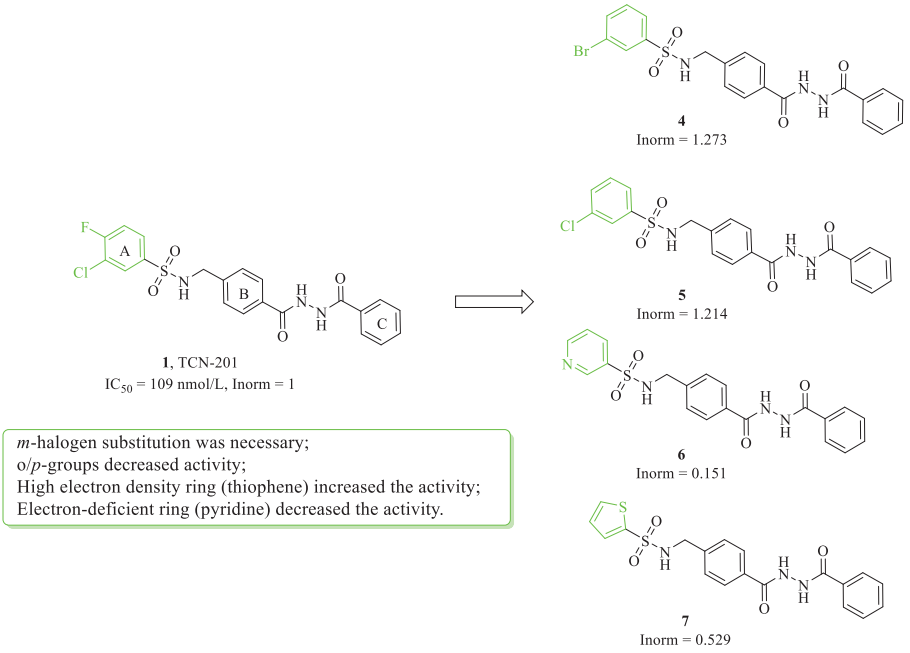

Figure 5 Lead compound TCN-201 and general SAR observations of ring A[85].

exhibited weaker activity, whereas thiophene-substituted analogues demonstrated higher activity due to their greater aromaticity.

Additionally, the substitution of phenyl ring C with an electron-deficient six-membered pyrimidin-4 ring and the presence of a short alkyl chain containing carboxylic acid or morpholine led to a reduction in activity. These observations are consistent with the hypothesis of cation−π interaction between the ligands and Arg755 (Fig. 3).

Furthermore, bulky fusion heteroaromatic ring substitutions were also investigated at this position. The introduction of indole-2- or indole-3-substitution significantly enhanced antagonistic activity (**12**, Inorm = 1.28). However, naphthalene or benzothiophene analogues exhibited weaker inhibitory activity, suggesting steric hindrance from surrounding residues with these ligands.

2.1.5. *Modifications on dihydrazide part*

Any modifications made to dihydrazide part could result in a decrease in potency profiles[85], clearly indicating the significant contribution of the dihydrazide part to the inhibitory activity of TCN-201 (Fig. 9). The introduction of methylene spacer (**13**, Inorm = 0.64) between the carbonyl group and phenyl ring C, replacement of the carbonyl group with sulfonyl bioisometry (**14**, Inorm = 0.58), or substitution of the dihydrazide part by bioisometric 1,3,4-oxadiazole ring (**15**, Inorm = 0.31) would lead to a notable reduction in activity. The decline in activity may be attributed to weakening cation−π interaction between the aromatic system and Arg755 guanidine group (GluN1A, Fig. 3)[79].

2.2. *Pyrazinamide analogues*

The compound TCN-201 exhibited a high level of selectivity for inhibiting GluN1/2A-containing NMDA receptor subunits. However, its inherent properties limited its potential for studying the pharmacology of GluN1/2A subunits in native systems. Therefore, Volkmann et al. conducted a medicinal chemistry optimization campaign to overcome these liabilities and create new tools for investigating GluN1/2A physiology[90]. They designed more potent and soluble antagonists based on the general skeleton of TCN-201 (Fig. 10). By eliminating the hydrazide moiety, reducing the number of H-bond donors, and decreasing lipophilicity, they identified more drug-like molecules such as analogue **18**, MPX-004 (IC_{50} = 79 nmol/L) and analogue **21**, MPX-007 (IC_{50} = 27 nmol/L, Fig. 11).

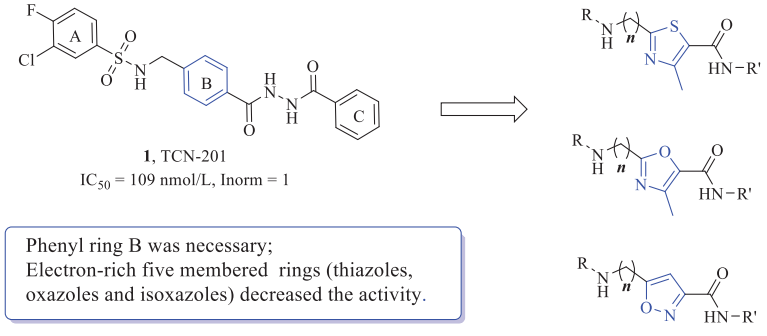

Figure 6 Lead compound TCN-201 and general SAR observations of ring B[82].

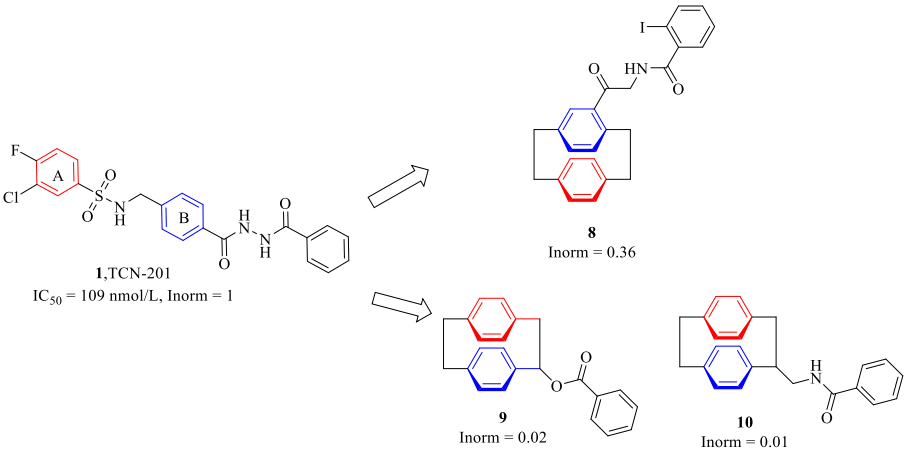

Figure 7 Lead compound TCN-201 and representative [2.2]paracyclophanes compounds[87,88].

After careful examination of residues surrounding the MPX binding site, it was observed that the GluN2A side chains underwent a conformation change to accommodate NAM binding. The most notable difference was observed in the repositioning of Val783 at the tip of the J-helix in GluN2A. It is known from literature[90] that the incremental displacement of GluN2A Val783 side chains, similar to NAMs (*i.e.*, TCN-201 < MPX004 < MPX-007), has significant potency and efficacy. The largest shift in GluN2A Val783 occurs when bound with MPX-007 (Fig. 11). The presence of GluN2A Val783 side chain prevents rotation of pyrazine ring B in MPX-007. At higher glycine concentrations, wider displacement of GluN2A Val783 and concurrent interaction with GluN1 Phe754 in MPX-007 compared to TCN-201 and MPX004 may account for the increased efficacy of MPX-007[79].

The dihydrazide moiety of TCN-201 played a crucial role in the inhibitory activity of GluN1/2A. However, Robert et al. initially substituted the phenyl hydrazide portion with 2-(methylthiazole-5-yl)methane amine, resulting in analogue **16** (IC_{50} = 398 nmol/L), which exhibited selective GluN1/2A NAM activity comparable to that of TCN-201. Subsequently, they replaced the carbon atom at different positions within the aromatic benzene ring with a nitrogen atom. Pyridine analogue **17** (IC_{50} = 75 nmol/L) containing a single nitrogen atom, displayed stronger inhibitory activity against GluN1/2A, while pyrazine analogue **18** (IC_{50} = 79 nmol/L) and **19** (IC_{50} = 166 nmol/L), incorporating two nitrogen atoms, maintained higher inhibitory activity and improved ADME characteristics. Introduction of a methyl group into the pyrazine nucleus resulted in compounds **20** (IC_{50} = 18 nmol/L) and **21** (IC_{50} = 29 nmol/L), furtherly enhancing efficacy compared to TCN-201. MPX-007 demonstrated superior effectiveness over MPX-004 due to the presence of a methyl group on its pyrazine nucleus. Further evaluation indicated that improvements in physicochemical and ADME properties for these compounds compared to TCN-201.

Moreover, they utilized high concentrations of Gly in the experimental exogenous expression system and observed that pyrazinamide analogues effectively and completely inhibited the activity of GluN1/2A. MPX-004 also inhibited the GluN1/2A component in NMDA receptor response in brain slices. Hence, even at elevated physiological Gly concentration, these analogues exhibited significant potency and selectivity in their interaction with receptor molecules. It is noteworthy that there was a slight difference in selectivity between MPX-004 and MPX-007 as observed in the oocyte test. These two compounds had no impact on GluN2C and GluN2D activities when completely inhibiting GluN1/2A activity. However, MPX-007 displayed weak but concentration-dependent inhibition on GluN2B activity, while MPX-004 did not exhibit obvious inhibition on GluN2B activity. The disparity between two compounds can be attributed to the halogen substituent on the phenylsulfonamide aromatic ring of MPX-007 and the methyl on the pyrazine nucleus. The SARs

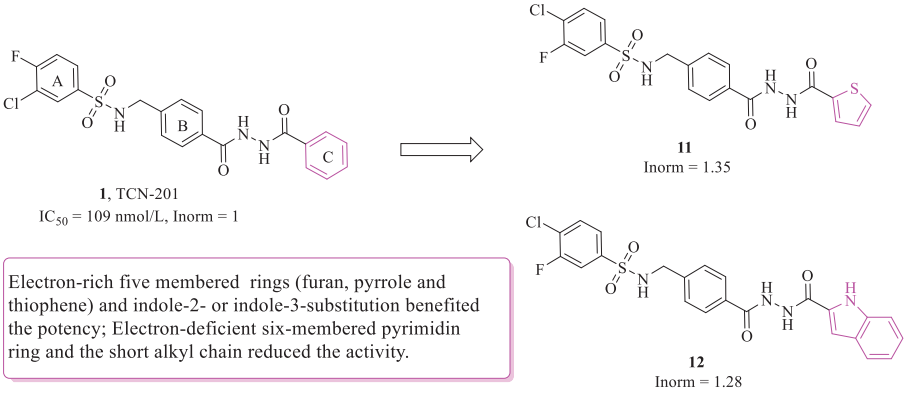

Figure 8 Lead compound TCN-201 and general SAR observations of ring C[85].

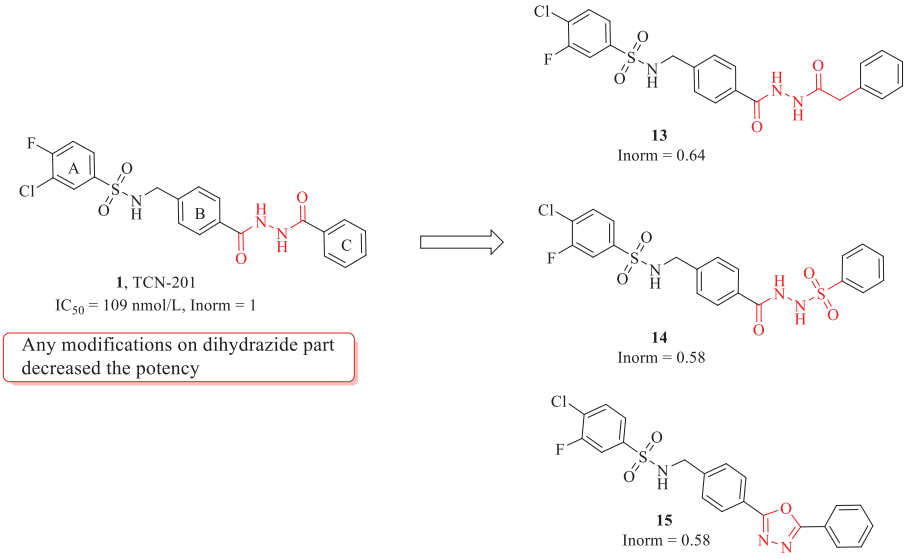

Figure 9 Lead compound TCN-201 and general SAR observations of dihydrazide part[79].

effect of GluN1/2A within these two regions is highly sensitive to various substitutions. Future research should focus more on recognizing additional binding sites for MPX and understand its mechanism of action along with regulatory Gly binding sites[79].

3. Selective GluN2A-containing NMDA receptors PAMs

In recent years, selective GluN1/2A PAMs have been discovered with reasonable efficacy and drug-like characteristics. These PAMs specifically bind to the dimer interface of GluN1/GluN2 ABD, thereby stabilizing the closed conformation and facilitating ligand binding[91–99].

3.1. Thiazole pyrimidinone analogues

In 2016, Hackos et al. identified a series of thiazole pyrimidinone analogues as selective PAMs for GluN2A-containing NMDA receptors (Fig. 13)[100]. To screen compounds that enhance the activation of NMDA receptors on Glu application in the presence of saturated Gly, they established a cell-based Ca^{2+} influx assay using HEK293 cells stably expressing GluN1 and GluN2A. A library containing 1.4 million compounds were tested, and analogues represented by compound **22** (GNE-3476, Fig. 13) were identified as effective PAMs for GluN1/2A. Further modification by Volgraf et al. resulted in compounds with this scaffold possessed good selectivity to GluN1/2A, and compound **23** (EC_{50} = 0.9 μmol/L) showed the best activity[95].

The structural biology investigation revealed that these molecules bind the dimer interface of GluN1/2A ABD, which exhibits significant structural similarity to the corresponding binding site of AMPA receptors. Consequently, thiazole pyrimidinone analogues also exhibit moderate activity towards AMPA receptors[101,102]. As depicted in Fig. 12, the binding pockets of AMPA receptors are relatively smaller compared to those of

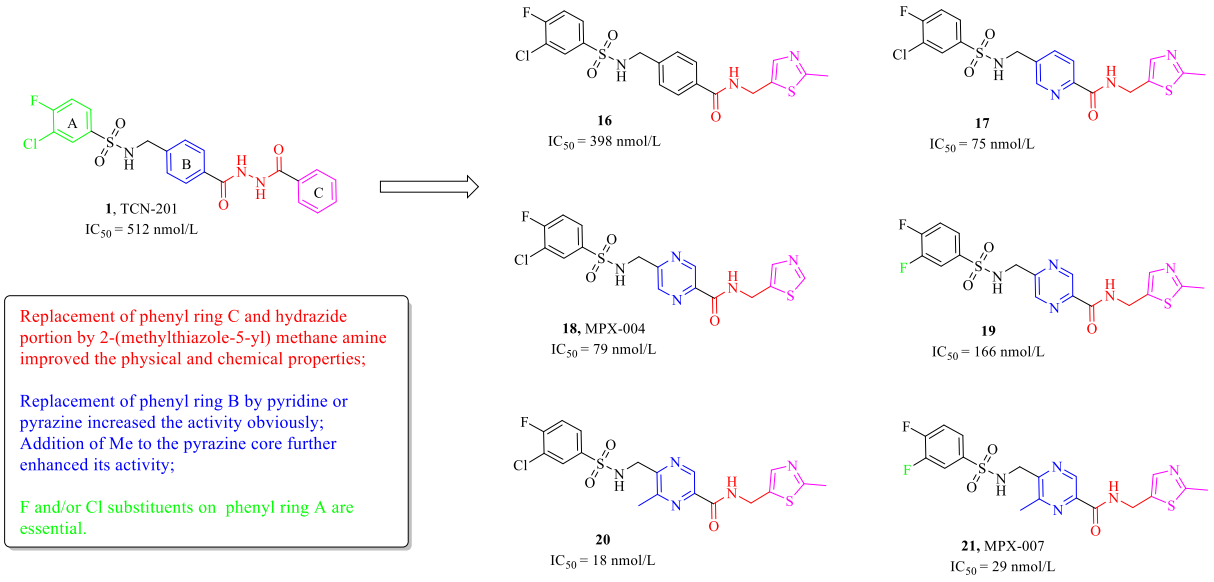

Figure 10 Lead compound TCN-201, representative compounds MPX-004, MPX-007 and general SAR observations.

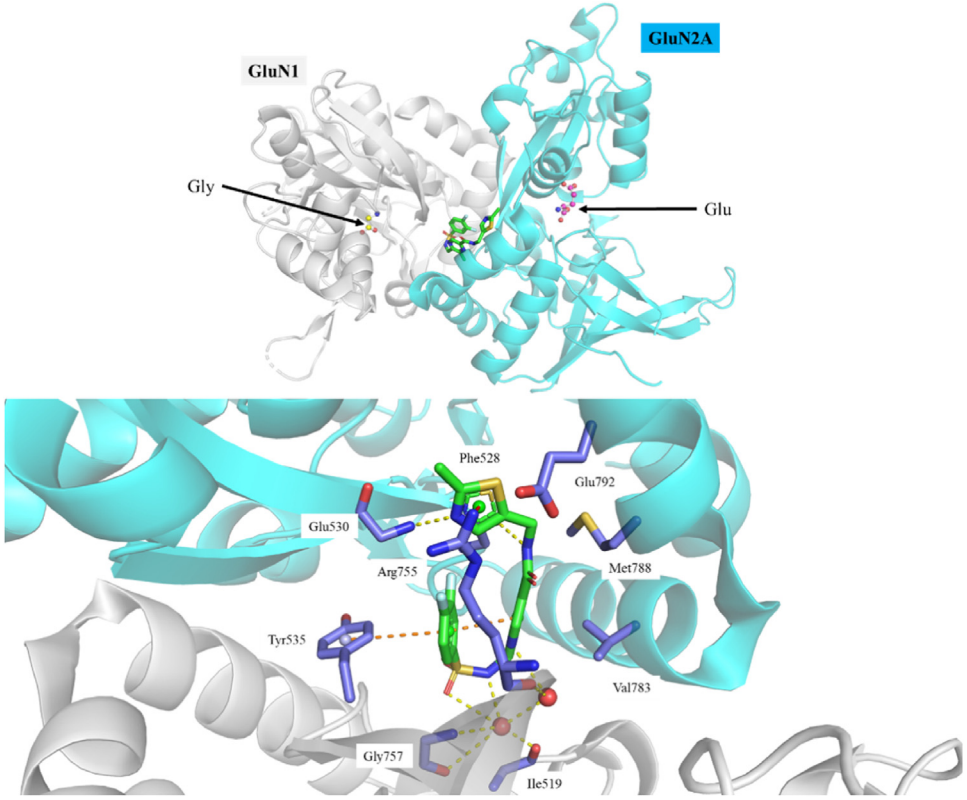

Figure 11 Binding mode of MPX-007 (GluN1: white cartoon; GluN2A: cyan cartoon; MPX-007: green stick; representative residues: blue stick; hydrogen bond: yellow dashed line; $\pi-\pi$ stacking: orange dashed line; cation$-\pi$ stacking: red dashed line. PDB code: 5I59)[79].

NMDA receptor. The residues of GluN2A possess smaller side chain when compared to those in AMPA receptor. Therefore, a substantial substitution at this binding site has the potential to determine selectivity between NMDA and AMPA receptors[94].

The cocrystal structure of compound **23** is depicted in Fig. 12, revealing its presence in both the NMDA receptor and AMPA receptor with distinct cavity sizes.

In order to achieve desirable selectivity, thiazole was employed as a substitution for the core of thiadiazole, with the substituent replacing the C′ terminus (Fig. 13). Biological evaluation revealed a slight improvement in overall efficiency upon replacing thiadiazole

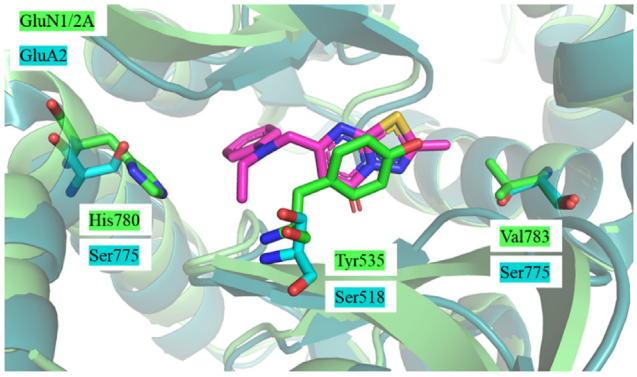

Figure 12 Binding mode of the difference of spatial position of the same ligand in NMDA receptor and AMPA receptors (PDB code: 5H8H, 5H8S)[90]. GluN2A, and key residues are color coded green, while GluA2 and key residues are color coded cyan.

with thiazole (Fig. 13). Substituting the C′-subunit of thiazole with heteroaryl rings, such as pyridine and pyrimidine, led to enhanced efficacy observed in compound **24** (EC_{50} = 0.168 μmol/L). Conversely, saturated heteroarenes like morpholine exhibited poor tolerance as demonstrated by compound **25** (EC_{50} = 2.2 μmol/L). The introduction of polar groups such as nitriles (compound **26**, EC_{50} = 0.129 μmol/L) and various aliphatic alcohols improved GluN1/2A effectiveness through substitution and interaction with the water network of the C′-subunit. Additionally, isopropene compound **27** (EC_{50} = 0.060 μmol/L) and methyl ketone were found to enhance GluN1/2A selectivity due to their π-character induced by the double bond.

The P-gp efflux ratio (<3) is a fundamental property shared by all CNS drugs[95,41]. It was observed that, with the exception of compound **28** (EC_{50} = 0.093 μmol/L, P-gp efflux ratio = 5.1), the P-gp efflux ratio of all analogues was below 3. Considering the enhanced potency and selectivity but poor P-gp efflux ratio of compound **29**, further optimization was conducted on the aniline position. The co-crystal structure of GluN1/2A ABD and ligands were explored (PDB code: 5KDT), respectively. Various aryl and heteroaryl groups were investigated, leading to the identification of 3-trifluoromethylpyrazole analogue **30** (EC_{50} = 0.436 μmol/L) as a promising candidate. Simulation results indicate that the *N*-ethyl motif of the lead compound binds to the same pocket as the C′-subsite group.

The subsequent investigation of different groups revealed that compound **31**, with the ethylamide substitution at the C′-subsite and a 5-chloro part, exhibited improved activity and selectivity towards GluN1/2A. However, it also resulted in an increased P-gp efflux ratio. Achieving a balance between activity,

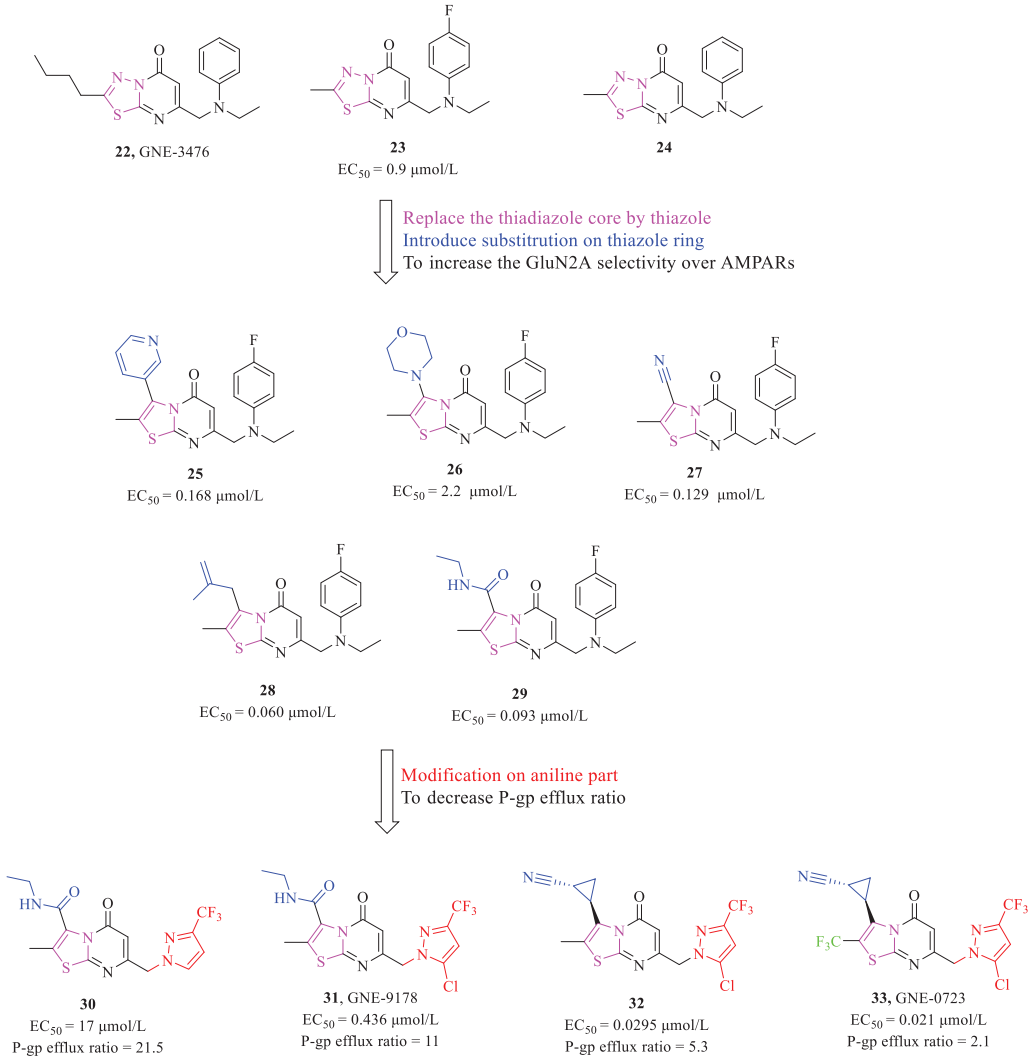

Figure 13 Lead compound **23,** representative compounds and general SAR observations[95].

selectivity, metabolic stability and blood−brain barrier (BBB) penetration has proven to be challenging. Nevertheless, this equilibrium was attained by introducing cyclopropyl nitrile substituents at the 3-position of the thiazole ring (**32**, EC_{50} = 0.0295 μmol/L, P-gp efflux ratio = 5.3). However, there still remained a high P-gp efflux ratio. Subsequently, a trifluoromethyl group was added to the 2-position of the thiazole nucleus (**33**, GNE-0723, EC_{50} = 0.021 μmol/L, P-gp efflux ratio = 2.1). This modification enhanced the metabolic function while increasing selectivity towards AMPA receptors without affecting efficiency. GNE-0723 was identified as a potent PAM selective for GluN1/2A with BBB penetrability for further *in vivo* characterization.

The cocrystal structure of GNE-0723 with GluN1/2A ABD illustrated that the unique binding conformation of *trans*-cyclopropyl enabled the nitrile group entering the distal water-filled pocket of C′-subunit. The pyrimidinone and pyridine substitution formed $\pi-\pi$ stacking interaction with Tyr535 and His780, respectively. Additionally, the chlorine atom formed a halogen bond with co-crystal water. The hydrophobic interaction between the transcyclopropyl and Val783 plays a crucial role in its selectivity for GluN1/2A over GluN1/2B (Phe), GluN1/2C (Leu), and GluN1/2D (Leu) residues (Fig. 14).

Although GNE-0723 exhibited high potency and subtype preference for the GluN1/2A, it possessed unfavorable pharmacokinetic properties (clearance rate in mice, CL = 26 mL/(min·kg); oral bioavailability, F = 24%). In 2016, Villemure et al. developed a series of analogues with a pyrido[1,2-*a*]pyrimidin-4-one scaffold (Fig. 15)[103]. The substitutions on the pyrimidine moiety were further investigated. Analogue **35** lacking the Me motif demonstrated approximately twofold improvement in activity compared to analogue **34** (GNE-3500, EC_{50} = 0.024 and 0.041 μmol/L, respectively). Small substituents such as fluorine atom displayed similar GluN1/2A potency. Moreover, the methoxy-substituted analogue (compound **36**, EC_{50} = 0.080 μmol/L) was three times less potent than GNE-0723. The chlorine substituent compound GNE-5729 (**37**, EC_{50} = 0.037 μmol/L) exhibited comparable potency to analogue **35** while significantly enhancing stability in human liver microsomes. In addition, compound **37** showed lower the efflux ratio (clearance rate in mice, CL = 10 mL/(min·kg);

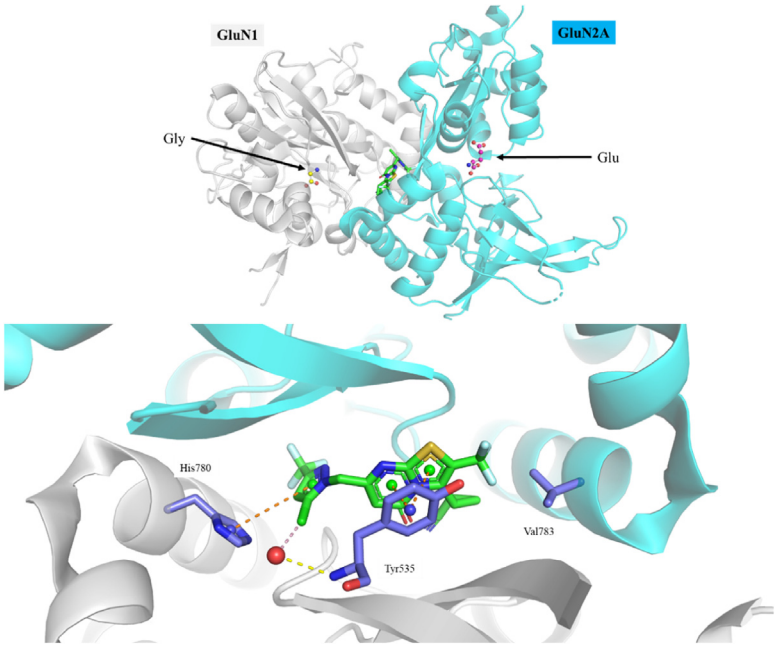

Figure 14 Binding mode of GNE-0723 with GluN1/2A ABD (GluN1: white cartoon; GluN2A: cyan cartoon; GNE-0723: green stick; Representative residues: blue stick; hydrogen bond: yellow dashed line; $\pi-\pi$ stacking: orange dashed line; halogen bond: pink dashed line. PDB code: 5KDT)[89].

bioavailability, $F = 37\%$), thereby increasing its potential to achieve biologically relevant free brain concentration *in vivo*. The neighboring site R_4 was also explored. However, no improvements in potency were observed for any decorations (methyl, methoxy or trifluoromethyl, etc.) analogues when R_3=H.

The pyridine pyrimidine ring and Tyr535, as well as pyrazole ring and His783, form $\pi-\pi$ stacking contacts, as depicted in Fig. 15B. Additionally, the chlorine atom forms a water bridge with Tyr535.

3.2. *Pyrazolo[1,5-a]pyrazin-4-one analogues*

In 2021, Sakurai et al. developed a series of analogues featuring the pyrazolo[1,5-*a*]pyrazin-4-one scaffold as GluN1/2A PAMs without exhibiting any binding affinity towards AMPA receptors (Fig. 16)[104].

The initial high-throughput screening, based on Ca^{2+} influx assay, identified a compound exhibiting internal AMPA receptors activity and also demonstrating moderate activity towards NMDA receptors (270% activation at 30 μmol/L). To minimize the binding activity to AMPA receptors and enhance GluN1/2A activity, a rational computer-aided drug design (CADD) method was employed.

The GluN1/2A activity can be enhanced by strengthening the $\pi-\pi$ interaction with Tyr144 and filling the space around the thiophene ring of the hit. Therefore, a series of analogues with thienopyridone and pyrazolopyrazinone scaffolds were designed, resulting in compounds **38** (EC_{50} = 2.3 μmol/L) and **39** (EC_{50} = 5.2 μmol/L) with improved activity towards NMDA receptors. Furthermore, introducing a methyl group on the central core analogues **40** (EC_{50} = 0.18 μmol/L) and **7** (EC_{50} = 0.16 μmol/L) not only increased their activity towards NMDA receptors but also significantly enhanced selectivity against AMPA receptors. Unfortunately, none of them exhibited acceptable metabolic stability. In addition, *in vitro* metabolite identification revealed that *n*-ethylaniline motif of compound **41** was partially oxidized and metabolized by rat liver microsomes. Moreover, it was found that the cyanoethyl side chain could only enhance GluN1/2A PAM activity in the presence of small substituents. Therefore, to address these issues, a methyl group was introduced on cyanoethyl side chain and replaced the phenyl ring with a 5-chloropyrazole ring which is known for its metabolic stability and wide application in previous analogues. These rational medicinal chemistry designs led to promising compound **42** (EC_{50} = 0.51 μmol/L), which demonstrated desirable GluN1/2A subtype selectivity, minimal off-target spectrum binding to AMPA receptors, as well as excellent brain permeability.

3.3. *Benzofuran analogues*

Coaviche-Yoval et al. discovered that compound **43** (*trans*-2,3-dihydrobenzofuran) and its derivatives exhibit protective effects against epileptic seizures, indicating their potential as NAMs of NMDA receptors[105]. Conversely, previous research has suggested that compound **44** and its racemic derivative **46** (*cis*-2,3-dihydrobenzofuran) act as the PAMs of the NMDA receptors. The authors furtherly proposed that **43** and derivative **45** are NAMs specific to Glu2A-containing NMDA receptors, while their regional isomers function as PAMs (Fig. 17). However, additional studies are required to elucidate the precise biological mechanism and selectivity of PAMs and NAMs.

3.4. *Furan-2-carboxamide analogues*

In 2021, Li et al. identified a series of NMDA PAMs with a furan-2-carboxamide scaffold by virtual screening. Notably, compound **47**, FS2921 (EC_{50} = 8.8 μmol/L, $\Delta I/I_{NMDA}$ = 3.2)

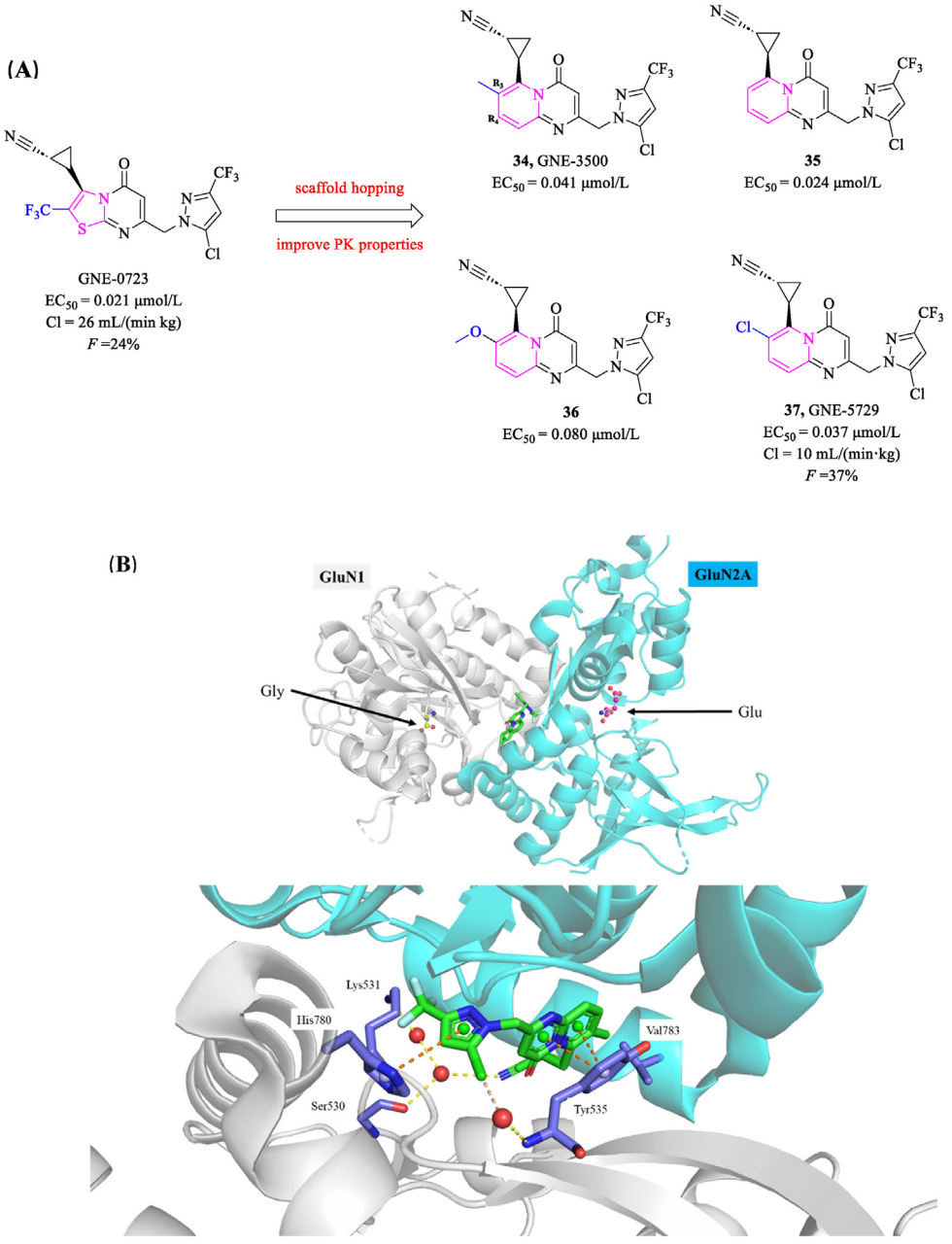

Figure 15 (A) Lead compound GNE-0723, representative compounds and general SAR observations. (B) Binding mode of GNE-3500 with GluN1/2A ABD (GluN1: white cartoon; GluN2A: cyan cartoon; GNE-3500: green stick; Representative residues: blue stick; hydrogen bond: yellow dashed line; $\pi-\pi$ stacking: orange dashed line; halogen bond: pink dashed line. PDB code: 5TPA)[103].

and compound **48**, FS2915 ($\Delta I/I_{NMDA}$ = 3.5, Fig. 18) were representative compounds discovered in this study[106]. Subsequent structure investigation focused on these two hits revealed that the removal of the pyrazol ring led to a loss of potentiating activity. SAR studies demonstrated the crucial role of the 3,5-dimethyl-1-pyrazol-1-yl group and *p*-substitution on phenyl ring for maintaining activity; moreover, larger decorations were also tolerated as seen in compounds **50** ($\Delta I/I_{NMDA}$ = 4.7) and **51** ($\Delta I/I_{NMDA}$ = 6.7). Replacement of the methyl group with a trifluoromethyl group resulted in improved potentiating activity observed in compounds **52** ($\Delta I/I_{NMDA}$ = 6.7) and **53** (EC_{50} = 12.5 μmol/L, $\Delta I/I_{NMDA}$ = 6.7). Furthermore, by transforming the furan ring of FS2921 into a thiophene ring, a series of novel analogues with a thiophene-carboxylamide scaffold was developed. These analogues exhibited higher stability and lower toxicity, and were represented by **54** (EC_{50} = 2.4 μmol/L, $\Delta I/I_{NMDA}$ = 6.7) and **55** (EC_{50} = 3.6 μmol/L, $\Delta I/I_{NMDA}$ = 14.3). Notably, the compound **54** demonstrated desirable PK/PD characteristics including moderate drug exposure, good brain penetration, low cytotoxicity, low hERG inhibition and suitability for long-term administration. Furthermore, it showed similar profile to Duloxetine in forced swimming test, suggesting its potential as a promising candidate for treating depression.

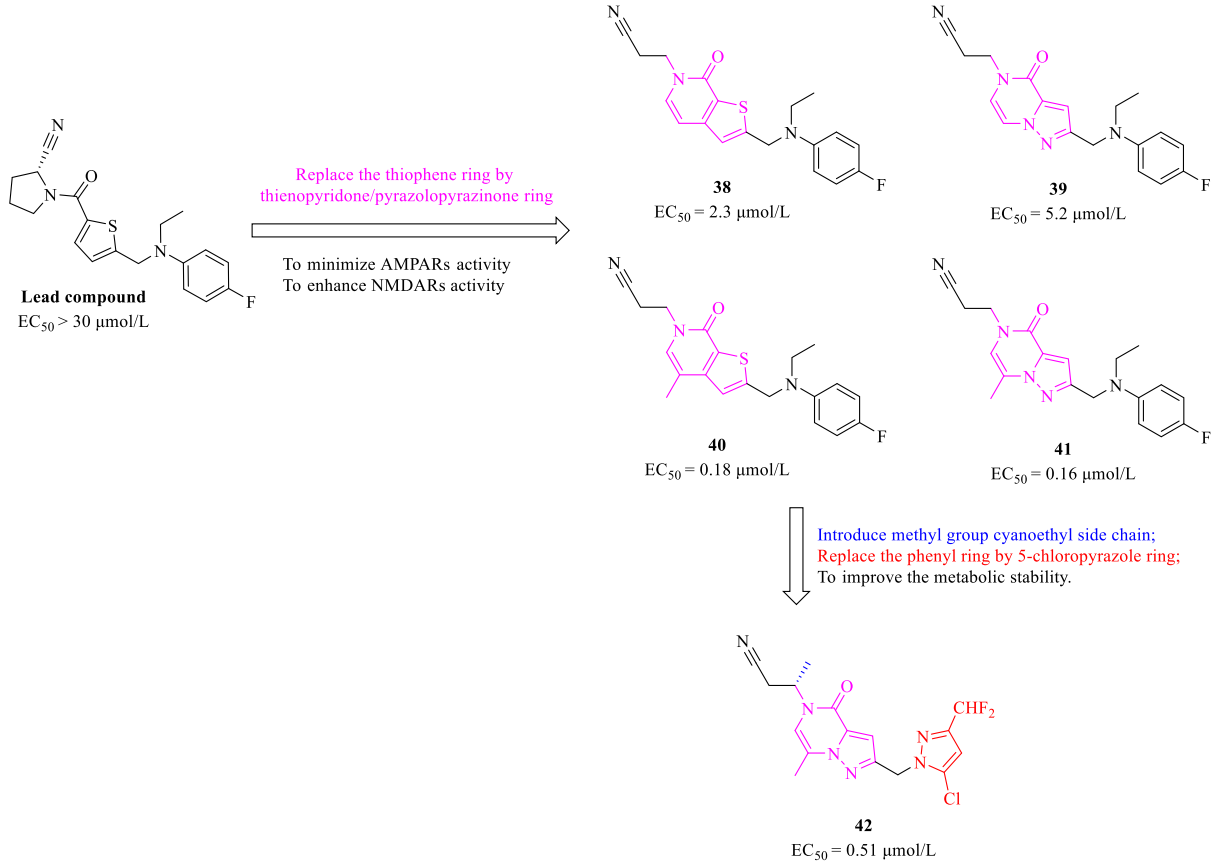

Figure 16 Lead compound, representative compounds and general SAR observations[99].

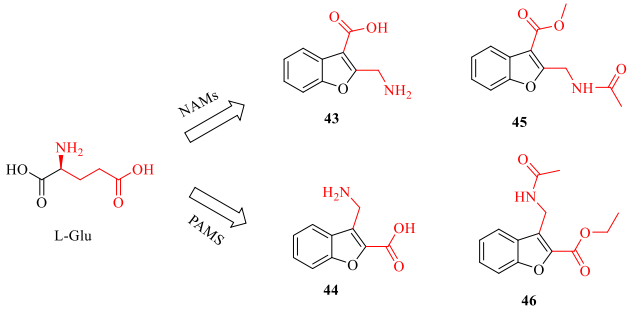

Figure 17 Lead compound L-Glu and representative compounds[100].

3.5. *Benzohydrazide analogues*

The compound **56**, Npam 43 (EC_{50} = 0.27 μmol/L) was identified as GluN1/2A PAM through virtual screening targeting the GluN1/2A ABD interface (Fig. 19)[107]. Importantly, Npam 43 demonstrated the ability to attenuate neuronal damage and enhance behavioral performance in rats with arterial occlusion after stroke. It might be worth noting that the compound contains a photoswitchable moiety (the cyan part of Fig. 19).

Generally, the GluN1/2A allosteric modulators can be divided into NAMs and PAMs (Fig. 20). TCN-201 and TCN-213, originally identified as the GluN1/2A antagonist, showed desirable subtype selectivity, but the poor pharmacological profiles prevent their application. MPX-007 improved the potency with better pharmacological profiles. GNE-0723 and GNE-5729 are the representative analogues of GluN1/2A PAMS and GME-5279 showed better clearance rate and oral bioavailability.

4. GluN1/2A subtype selective antagonists

4.1. *Dihydroxyquinoxaline analogues*

In 2002, Auberson et al. discovered compound **57** as a potent, non-chiral, and oral active NMDA antagonist with a preference for GluN1/2A (Fig. 21)[108–110]. Further optimization efforts focused on the *meta*-position of phenyl ring, revealing that this position's activity was not sensitive to improvement. The introduction of larger groups such as benzylamine or cyclohexyl methyl resulted in lower nanomolar binding affinity. Ultimately, compound **58**, NVP-AAM077 (IC_{50} = 68.4 nmol/L), an antagonist known as NVP-AAM077 with an additional methyl group, was identified to exhibit a 100-fold selectivity for GluN1/2A. However, further investigation revealed a 12-fold preference for GluN1/2A over GluN2B and no concentration range allowed complete inhibition of the GluN1/2A receptor without affecting the GluN2B receptor.

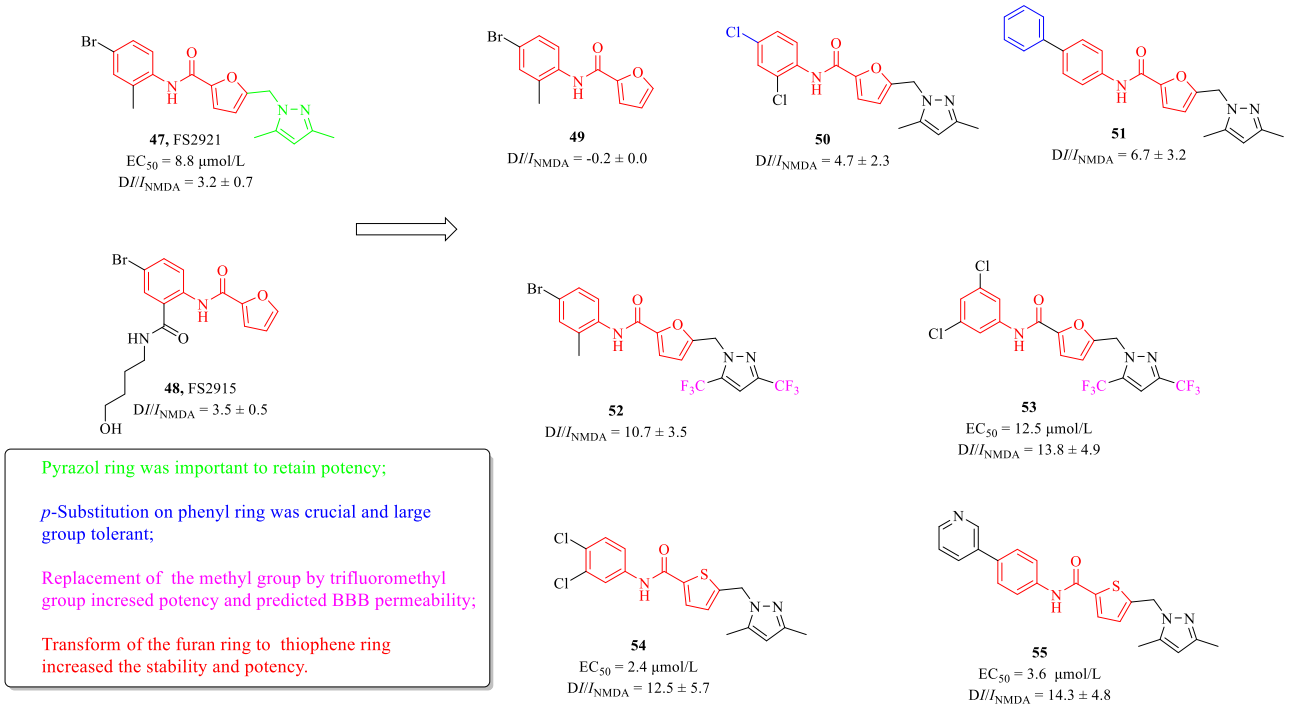

Figure 18 Lead compound FS2921 and representative compounds and general SAR observations[101].

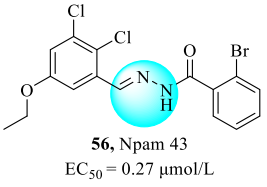

Figure 19 Representative compound Npam 43[102]. The cyan part indicates the photo-switchable moiety.

The inhibitory effect of NVP-AM077 largely depends on the effective Glu concentration which is typically unknown in physiological experiments and likely varies under different stimulus regimens.

As shown in Fig. 22, NVP-AAM077 bound the Glu binding site of GluN2A. The phosphate group establishes multiple hydrogen bonds and water bridges with neighboring residues. Additionally, the extra Br-phenyl motif aligns towards the interface of GluN1 and GluN2A[108].

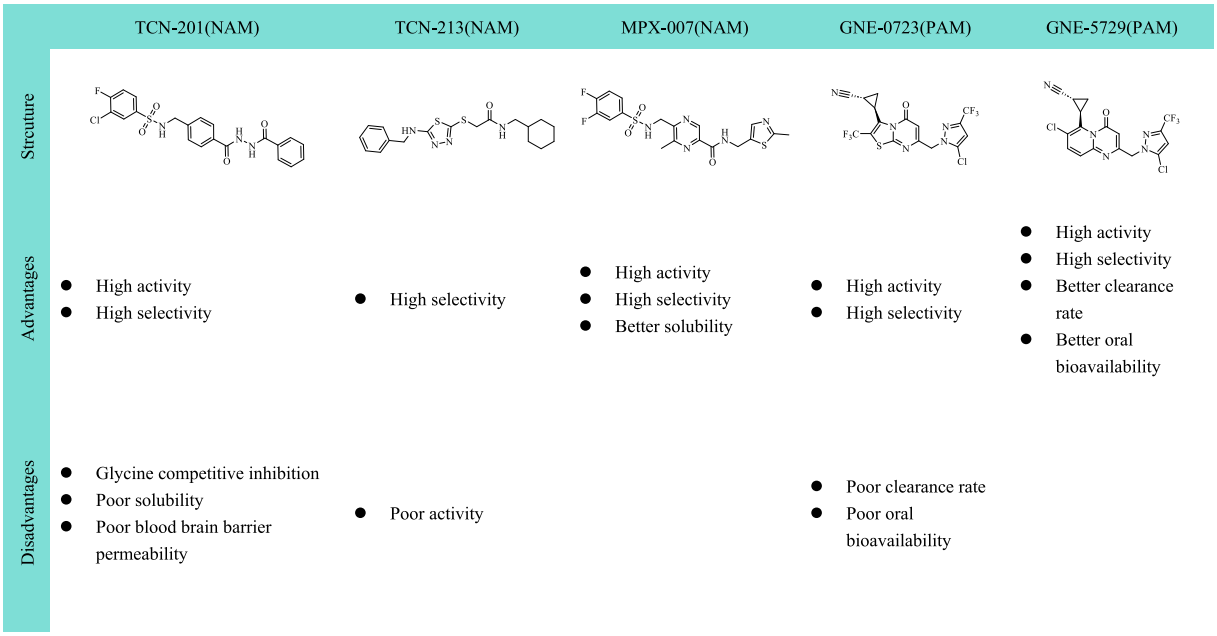

Figure 20 The representative PAM and NAM advantages and disadvantages[79,82,83,95,103].

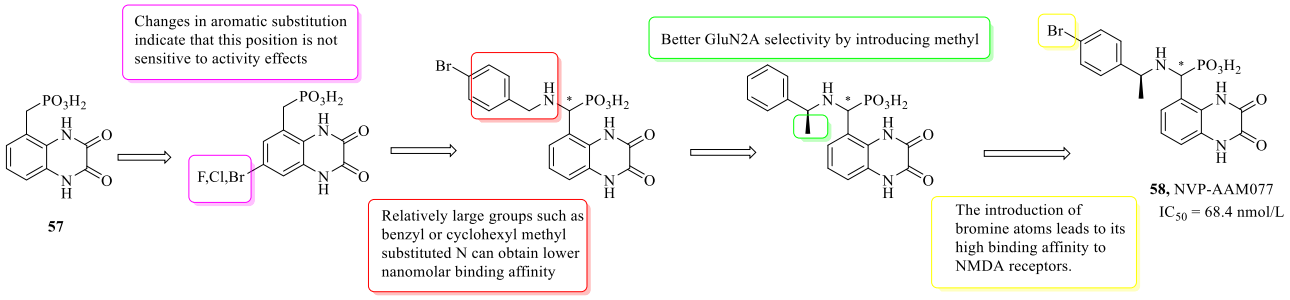

Figure 21 Lead compound **57** and general SAR observations[105].

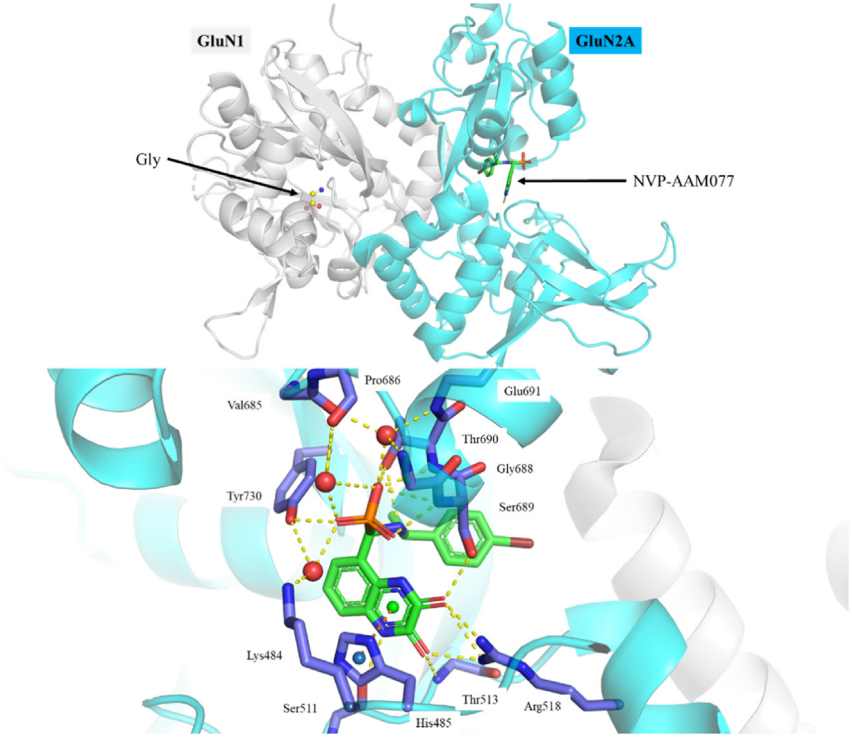

Figure 22 Binding mode of NVP-AAM077 with GluN1/2A ABD (GluN1: white cartoon; GluN2A: cyan cartoon; **58**: green stick; Representative residues: blue stick; hydrogen bond: yellow dashed line; $\pi-\pi$ stacking: orange dashed line. PDB code: 5U8C)[103].

4.2. *Dihydroisoxazole analogues*

In 2004, Conti et al. reported the synthesis and pharmacological characterization of compound **59**, F94b and compound **60**, F94c (Fig. 23)[111,112], which exhibited potent antagonistic effects on NMDA receptors. In 2010, further modification was performed based on these two antagonists by replacing the original isoxazoline ring with a pyrazoline ring and introducing a phenyl ring with or without substitution. These new analogues displayed preference for GluN1/2A and GluN1/2B subtypes over GluN1/2C and GluN1/2D. Among them, compound **61** (IC_{50} = 320 nmol/L) demonstrated nanomolar affinity to NMDA receptors. In 2017, Tamborini et al. also incorporated *p*-halogen onto the phenyl ring resulting in analogues that showed preference for the GluN1/2A, exemplified by compound **62**, 4C (IC_{50} = 91 nmol/L). Furthermore, Lind et al. explored longer chain on *p*-position, and led to a specific antagonist compound **63**, ST-3 (K_i = 51.8 and 782 nmol/L to GluN1/2A and GluN1/2B, respectively) with 15-fold preference to GluN1/2A over GluN1/2B[109].

The binding of ST-3 to the GluN1/2A, similar to NVP-AAM077[109], was observed at the Glu binding site (Fig. 24). The amino acid group formed multiple hydrogen bonds and water bridges with surrounding residues, while the other carboxyl motifs also established several hydrogen bonds and water bridges with neighboring residues. Additionally, the phenyl ring oriented towards the interface between GluN1 and GluN2A.

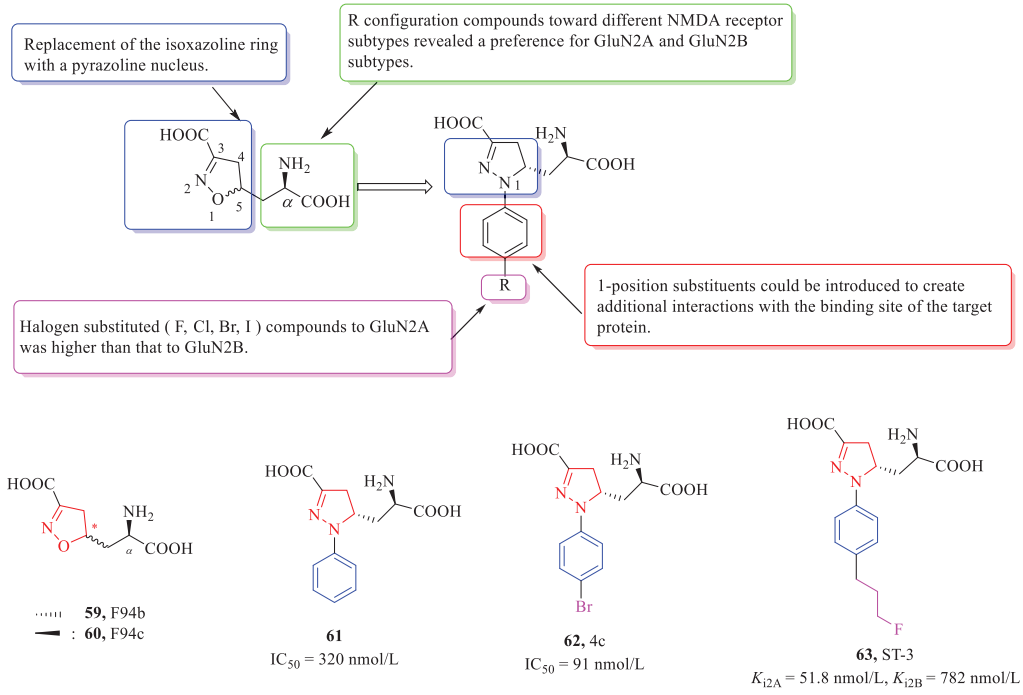

Figure 23 Lead compound F49b, representative compounds and general SAR observations[106,107].

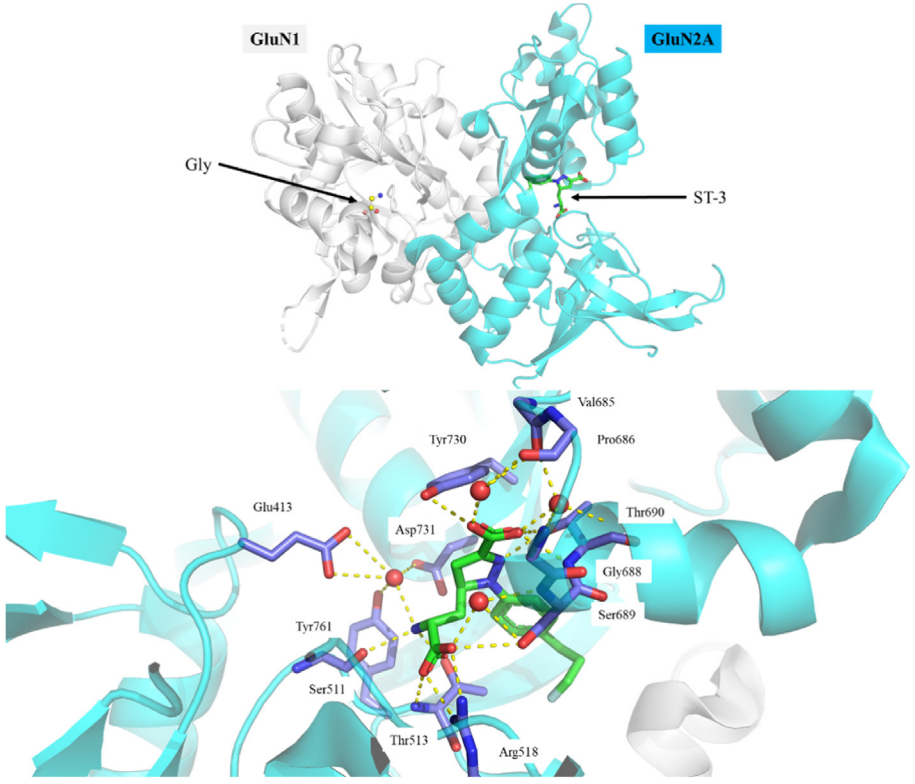

Figure 24 Binding mode of ST-3 with GluN1/2A ABD (GluN1: white cartoon; GluN2A: cyan cartoon; ST-3: green stick; representative residues: blue stick; hydrogen bond: yellow dashed line. PDB code: 5VII)[103].

5. Conclusions and perspectives

In recent years, significant advancements have been made in the investigation of newly discovered site binding on NMDARs. These novel binding sites have demonstrated immense potential as therapeutic targets and tools. The presence of multiple binding pockets suggests that identification of several subtypes of selective ligands with both enhancing and inhibiting activities. Although there are numerous compounds exhibiting sufficient pharmacological properties and serving as potential starting points for therapeutic research, further development of new compounds still necessary. Future research should prioritize (1) expanding the structural diversity of lead compounds, (2) enhancing pharmacodynamic properties by optimizing the balance between water solubility and lipophilicity (which has posed challenging in some SAR studies discussed in this paper) to improve bioavailability, (3) improving selectivity towards individual GluN2 subunits[113].

In this paper, we conducted a comprehensive review on the structure, development and SARs of GluN1/2A subtype selective ligands. Despite the discovery of several novel GluN1/2A subtype selective analogues, their efficacy in clinical trials has been limited. The main challenge lies in achieving clinically feasible and effective small molecules that specifically target the GluN1/2A subtype. Therefore, it remains challenging to discover selective GluN1/2A small molecules and successfully translate them into clinical practice.

The advancement of computer-aided design device[114], encompassing molecular and pharmacophore modeling, 3D-quantitative structure−activity relationship (3D-QSAR), absorption, distribution, metabolism, excretion, and toxicity (ADMET) prediction and artificial intelligence-based drug design, can provide enhanced impetus for the design and development of selective GluN1/2A ligands and may offer novel insights for future advancements in GluN1/2A-based small molecules research.

Acknowledgments

The work was supported by the National Natural Science Foundation of China (82204200), the International Postdoctoral Exchange Fellowship Program (Talent-Introduction Program, YJ20210279, China), the China Postdoctoral Science Foundation (2022M711939) to Fabao Zhao, and the Natural Science Foundation of Shandong Province (ZR2022QH287 to Fabao Zhao and ZR2022QH312 to Na Liu, China).

Author contributions

Original draft preparation: Liyang Jiang and Na Liu; review and editing: Na Liu, Fabao Zhao, Boshi Huang, Dongwei Kang, Peng Zhan, Xinyong Liu. All authors contributed to data collection and manuscript revision.

Conflicts of interest

The authors declare no conflict of interest.

References

1. Cruzat V, Macedo Rogero M, Noel Keane K, Curi R, Newsholme P. Glutamine: metabolism and immune function, supplementation and clinical translation. *Nutrients* 2018;**10**:1564−95.
2. Davani-Davari D, Karimzadeh I, Sagheb MM, Khalili H. The renal safety of L-carnitine, L-arginine, and glutamine in athletes and bodybuilders. *J Ren Nutr* 2019;**29**:221−34.
3. Martineau M. Gliotransmission: focus on exocytotic release of L-glutamate and D-serine from astrocytes. *Biochem Soc Trans* 2013;**41**:1557−61.
4. Traynelis SF, Wollmuth LP, McBain CJ, Menniti FS, Vance KM, Ogden KK, et al. Glutamate receptor ion channels: structure, regulation, and function. *Pharmacol Rev* 2010;**62**:405−96.
5. Stepulak A, Rola R, Polberg K, Ikonomidou C. Glutamate and its receptors in cancer. *J Neural Transm* 2014;**121**:933−44.
6. Niswender CM, Conn PJ. Metabotropic glutamate receptors: physiology, pharmacology, and disease. *Annu Rev Pharmacol Toxicol* 2010;**50**:295−322.
7. Falcón-Moya R, Rodríguez-Moreno A. Metabotropic actions of kainate receptors modulating glutamate release. *Neuropharmacology* 2021;**197**:108696.
8. Egbenya DL, Aidoo E, Kyei G. Glutamate receptors in brain development. *Childs Nerv Syst* 2021;**37**:2753−8.
9. Paoletti P, Bellone C, Zhou Q. NMDA receptor subunit diversity: impact on receptor properties, synaptic plasticity and disease. *Nat Rev Neurosci* 2013;**14**:383−400.
10. Hansen KB, Wollmuth LP, Bowie D, Furukawa H, Menniti FS, Sobolevsky AI, et al. Structure, function, and pharmacology of glutamate receptor ion channels. *Pharmacol Rev* 2021;**73**:298−487.
11. Xie D, Xiong K, Su X, Wang G, Ji Q, Zou Q, et al. Identification of an endogenous glutamatergic transmitter system controlling excitability and conductivity of atrial cardiomyocytes. *Cell Res* 2021;**31**:951−64.
12. Stroebel D, Mony L, Paoletti P. Glycine agonism in ionotropic glutamate receptors. *Neuropharmacology* 2021;**193**:108631.
13. Reiner A, Levitz J. Glutamatergic signaling in the central nervous system: ionotropic and metabotropic receptors in concert. *Neuron* 2018;**98**:1080−98.
14. Bowie D. The many faces of the AMPA-type ionotropic glutamate receptor. *Neuropharmacology* 2022;**208**:108975.
15. Liu W, Jiang X, Zu Y, Yang Y, Liu Y, Sun X, et al. A comprehensive description of GluN2B-selective *N*-methyl-D-aspartate (NMDA) receptor antagonists. *Eur J Med Chem* 2020;**200**:112447.
16. Greger IH, Watson JF, Cull-Candy SG. Structural and functional architecture of AMPA-type glutamate receptors and their auxiliary proteins. *Neuron* 2017;**94**:713−30.
17. Morris RG. NMDA receptors and memory encoding. *Neuropharmacology* 2013;**74**:32−40.
18. Koutsilieri E, Riederer P. Excitotoxicity and new antiglutamatergic strategies in Parkinson's disease and Alzheimer's disease. *Parkinsonism Relat Disorders* 2007;**13**:S329−31.
19. Kamat PK, Kalani A, Rai S, Swarnkar S, Tota S, Nath C, et al. Mechanism of oxidative stress and synapse dysfunction in the pathogenesis of Alzheimer's disease: understanding the therapeutics strategies. *Mol Neurobiol* 2016;**53**:648−61.
20. Hegoburu C, Parrot S, Ferreira G, Mouly AM. Differential involvement of amygdala and cortical NMDA receptors activation upon encoding in odor fear memory. *Learn Mem* 2014;**21**:651−5.
21. Bast T, da Silva BM, Morris RG. Distinct contributions of hippocampal NMDA and AMPA receptors to encoding and retrieval of one-trial place memory. *J Neurosci* 2005;**25**:5845−56.
22. Zhigulin AS, Barygin OI. Mechanisms of NMDA receptor inhibition by Nafamostat, Gabexate and Furamidine. *Eur J Pharmacol* 2022;**919**:174795.
23. Zhang Y, Ye F, Zhang T, Lv S, Zhou L, Du D, et al. Structural basis of ketamine action on human NMDA receptors. *Nature* 2021;**596**:301−5.
24. Vyklicky V, Korinek M, Smejkalova T, Balik A, Krausova B, Kaniakova M, et al. Structure, function, and pharmacology of NMDA receptor channels. *Physiol Res* 2014;**63**:S191−203.
25. Strong KL, Jing Y, Prosser AR, Traynelis SF, Liotta DC. NMDA receptor modulators: an updated patent review (2013−2014). *Expert Opin Ther Pat* 2014;**24**:1349−66.

26. Song X, Jensen M, Jogini V, Stein RA, Lee CH, McHaourab HS, et al. Mechanism of NMDA receptor channel block by MK-801 and memantine. *Nature* 2018;**556**:515−9.
27. Schrattenholz A, Soskic V. NMDA receptors are not alone: dynamic regulation of NMDA receptor structure and function by neuregulins and transient cholesterol-rich membrane domains leads to disease-specific nuances of glutamate-signalling. *Curr Top Med Chem* 2006;**6**:663−86.
28. Paoletti P, Neyton J. NMDA receptor subunits: function and pharmacology. *Curr Opin Pharmacol* 2007;**7**:39−47.
29. Lüscher C, Malenka RC. NMDA receptor-dependent long-term potentiation and long-term depression (ltp/ltd). *Cold Spring Harbor Perspect Biol* 2012;**4**:106133.
30. Leeson PD, Iversen LL. The glycine site on the NMDA receptor: structure−activity relationships and therapeutic potential. *J Med Chem* 1994;**37**:4053−67.
31. Flores-Soto ME, Chaparro-Huerta V, Escoto-Delgadillo M, Vazquez-Valls E, González-Castañeda RE, Beas-Zarate C. Structure and function of NMDA-type glutamate receptor subunits. *Neurologia* 2012;**27**:301−10.
32. Dannhardt G, Kohl BK. The glycine site on the NMDA receptor: structure−activity relationships and possible therapeutic applications. *Curr Med Chem* 1998;**5**:253−63.
33. Stein IS, Park DK, Claiborne N, Zito K. Non-ionotropic NMDA receptor signaling gates bidirectional structural plasticity of dendritic spines. *Cell Rep* 2021;**34**:108664.
34. Leszkiewicz DN, Kandler K, Aizenman E. Enhancement of NMDA receptor-mediated currents by light in rat neurones *in vitro*. *J Physiol* 2000;**524**:365−74.
35. Lee CH, Lü W, Michel JC, Goehring A, Du J, Song X, et al. NMDA receptor structures reveal subunit arrangement and pore architecture. *Nature* 2014;**511**:191−7.
36. Karakas E, Furukawa H. Crystal structure of a heterotetrameric NMD receptor ion channel. *Science* 2014;**344**:992−7.
37. Jessen M, Frederiksen K, Yi F, Clausen RP, Hansen KB, Bräuner-Osborne H, et al. Identification of aicp as a GluN2C-selective *N*-methyl-D-aspartate receptor superagonist at the GluN1 glycine site. *Mol Pharmacol* 2017;**92**:151−61.
38. Tajima N, Karakas E, Grant T, Simorowski N, Diaz-Avalos R, Grigorieff N, et al. Activation of NMDA receptors and the mechanism of inhibition by Ifenprodil. *Nature* 2016;**534**:63−8.
39. Romero-Hernandez A, Simorowski N, Karakas E, Furukawa H. Molecular basis for subtype specificity and high-affinity zinc inhibition in the GluN1−GluN2A NMDA receptor amino-terminal domain. *Neuron* 2016;**92**:1324−36.
40. Krzystanek M, Pałasz A. NMDA receptor model of antipsychotic drug-induced hypofrontality. *Int J Mol Sci* 2019;**20**:1442−59.
41. Černý J, Božíková P, Balík A, Marques SM, Vyklický L. NMDA receptor opening and closing-transitions of a molecular machine revealed by molecular dynamics. *Biomolecules* 2019;**9**:546−63.
42. Blandl T, Warder SE, Prorok M, Castellino FJ. Structure−function relationships of the NMDA receptor antagonist peptide, conantokin-r. *FEBS Lett* 2000;**470**:139−46.
43. Balu DT. The NMDA receptor and Schizophrenia: from pathophysiology to treatment. *Adv Pharmacol* 2016;**76**:351−82.
44. Amin JB, Moody GR, Wollmuth LP. From bedside-to-bench: what disease-associated variants are teaching us about the nmda receptor. *J Physiol* 2021;**599**:397−416.
45. Aepkers M, Wünsch B. Structure−affinity relationship studies of non-competitive NMDA receptor antagonists derived from dexoxadrol and etoxadrol. *Bioorg Med Chem* 2005;**13**:6836−49.
46. Babaei P. NMDA and AMPA receptors dysregulation in Alzheimer's disease. *Eur J Pharmacol* 2021;**908**:174310.
47. Ahmed H, Haider A, Ametamey SM. *N*-Methyl-D-aspartate (NMDA) receptor modulators: a patent review (2015−present). *Expert Opin Ther Pat* 2020;**30**:743−67.
48. Booker SA, Wyllie DJA. NMDA receptor function in inhibitory neurons. *Neuropharmacology* 2021;**196**:108609.
49. Davies JA. Mechanisms of action of antiepileptic drugs. *Seizure* 1995;**4**:267−71.
50. Karakas E, Simorowski N, Furukawa H. Subunit arrangement and phenylethanolamine binding in GluN1/GluN2B NMDA receptors. *Nature* 2011;**475**:249−53.
51. Gorecki L, Misiachna A, Damborsky J, Dolezal R, Korabecny J, Cejkova L, et al. Structure-activity relationships of dually-acting acetylcholinesterase inhibitors derived from tacrine on *N*-methyl-D-aspartate receptors. *Eur J Med Chem* 2021;**219**:113434.
52. Zhang Y, Wu J, Yan Y, Gu Y, Ma Y, Wang M, et al. Sapap3 regulates epileptic seizures involving GluN2A in post-synaptic densities. *Cell Death Dis* 2022;**13**:437.
53. Zhang XM, Luo JH. GluN2A versus GluN2B: twins, but quite different. *Neurosci Bull* 2013;**29**:761−72.
54. Sun Y, Zhan L, Cheng X, Zhang L, Hu J, Gao Z. The regulation of GluN2A by endogenous and exogenous regulators in the central nervous system. *Cell Mol Neurobiol* 2017;**37**:389−403.
55. Sun Y, Xu Y, Cheng X, Chen X, Xie Y, Zhang L, et al. The differences between GluN2A and GluN2B signaling in the brain. *J Neurosci Res* 2018;**96**:1430−43.
56. Sun Y, Cheng X, Hu J, Gao Z. The role of GluN2A in cerebral ischemia: promoting neuron death and survival in the early stage and thereafter. *Mol Neurobiol* 2018;**55**:1208−16.
57. Niu M, Yang X, Li Y, Sun Y, Wang L, Ha J, et al. Progresses in GluN2A-containing NMDA receptors and their selective regulators. *Cell Mol Neurobiol* 2023;**43**:139−53.
58. Li QQ, Chen J, Hu P, Jia M, Sun JH, Feng HY, et al. Enhancing GluN2A-type NMDA receptors impairs long-term synaptic plasticity and learning and memory. *Mol Psychiatr* 2022;**27**:3468−78.
59. Franchini L, Carrano N, Di Luca M, Gardoni F. Synaptic GluN2A-containing NMDA receptors: from physiology to pathological synaptic plasticity. *Int J Mol Sci* 2020:21.
60. Durante V, de Iure A, Loffredo V, Vaikath N, De Risi M, Paciotti S, et al. Alpha-synuclein targets GluN2A NMDA receptor subunit causing striatal synaptic dysfunction and visuospatial memory alteration. *Brain* 2019;**142**:1365−85.
61. Tran KN, Nguyen NPK, Nguyen LTH, Shin HM, Yang IJ. Screening for neuroprotective and rapid antidepressant-like effects of 20 essential oils. *Biomedicines* 2023;**11**:1248.
62. Thum S, Schepmann D, Kalinin DV, Ametamey SM, Wünsch B. Replacement of the benzylpiperidine moiety with fluorinated phenylalkyl side chains for the development of GluN2B receptor ligands. *ChemMedChem* 2018;**13**:2522−9.
63. Hardingham GE, Bading H. Synaptic *versus* extrasynaptic NMDA receptor signalling: implications for neurodegenerative disorders. *Nat Rev Neurosci* 2010;**11**:682−96.
64. Naassila M, Pierrefiche O. GluN2B subunit of the B NMDA receptor: the keystone of the effects of alcohol during neurodevelopment. *Neurochem Res* 2019;**44**:78−88.
65. Li DC, Pitts EG, Dighe NM, Gourley SL. GluN2B inhibition confers resilience against long-term cocaine-induced neurocognitive sequelae. *Neuropsychopharmacology* 2023;**48**:1108−17.
66. Tarrés-Gatius M, Miquel-Rio L, Campa L, Artigas F, Castañé A. Involvement of NMDA receptors containing the GluN2C subunit in the psychotomimetic and antidepressant-like effects of ketamine. *Transl Psychiatry* 2020;**10**:427.
67. Ravikrishnan A, Gandhi PJ, Shelkar GP, Liu J, Pavuluri R, Dravid SM. Region-specific expression of NMDA receptor GluN2C subunit in parvalbumin-positive neurons and astrocytes: analysis of GluN2C expression using a novel reporter model. *Neuroscience* 2018;**380**:49−62.
68. Obata Y, Ciofani G, Raffa V, Cuschieri A, Menciassi A, Dario P, et al. Evaluation of cationic liposomes composed of an amino acid-based lipid for neuronal transfection. *Nanomedicine* 2010;**6**:70−7.

69. Morris PG, Mishina M, Jones S. Altered synaptic and extrasynaptic NMDA receptor properties in substantia nigra dopaminergic neurons from mice lacking the GluN2D subunit. *Front Cell Neurosci* 2018;**12**:354.
70. Yi F, Rouzbeh N, Hansen KB, Xu Y, Fanger CM, Gordon E, et al. Ptc-174, a positive allosteric modulator of NMDA receptors containing GluN2C or GluN2D subunits. *Neuropharmacology* 2020;**173**:107971.
71. Wang JX, Irvine MW, Burnell ES, Sapkota K, Thatcher RJ, Li M, et al. Structural basis of subtype-selective competitive antagonism for GluN2C/2D-containing nmda receptors. *Nat Commun* 2020;**11**:423.
72. Swanger SA, Vance KM, Acker TM, Zimmerman SS, DiRaddo JO, Myers SJ, et al. A novel negative allosteric modulator selective for GluN2C/2D-containing nmda receptors inhibits synaptic transmission in hippocampal interneurons. *ACS Chem Neurosci* 2018;**9**:306−19.
73. Suryavanshi PS, Ugale RR, Yilmazer-Hanke D, Stairs DJ, Dravid SM. GluN2C/2D subunit-selective nmda receptor potentiator ciq reverses Mk-801-induced impairment in prepulse inhibition and working memory in y-maze test in mice. *Br J Pharmacol* 2014;**171**:799−809.
74. Shelkar GP, Pavuluri R, Gandhi PJ, Ravikrishnan A, Gawande DY, Liu J, et al. Differential effect of NMDA receptor GluN2C and GluN2D subunit ablation on behavior and channel blocker-induced schizophrenia phenotypes. *Sci Rep* 2019;**9**:7572.
75. Mao Z, He S, Mesnard C, Synowicki P, Zhang Y, Chung L, et al. NMDA receptors containing GluN2C and GluN2D subunits have opposing roles in modulating neuronal oscillations; potential mechanism for bidirectional feedback. *Brain Res* 2020;**1727**:146571.
76. Alsaad HA, DeKorver NW, Mao Z, Dravid SM, Arikkath J, Monaghan DT. In the telencephalon, GluN2C NMDA receptor subunit mRNA is predominately expressed in glial cells and GluN2D mRNA in interneurons. *Neurochem Res* 2019;**44**:61−77.
77. Wild AR, Akyol E, Brothwell SL, Kimkool P, Skepper JN, Gibb AJ, et al. Memantine block depends on agonist presentation at the NMDA receptor in substantia nigra pars compacta dopamine neurones. *Neuropharmacology* 2013;**73**:138−46.
78. Wu YN, Johnson SW. Memantine selectively blocks extrasynaptic NMDA receptors in rat substantia nigra dopamine neurons. *Brain Res* 2015;**1603**:1−7.
79. Zhao F, Atxabal U, Mariottini S, Yi F, Lotti JS, Rouzbeh N, et al. Derivatives of (*r*)-3-(5-furanyl)carboxamido-2-aminopropanoic acid as potent NMDA receptor glycine site agonists with GluN2 subunit-specific activity. *J Med Chem* 2022;**65**:734−46.
80. Zhao F, Mazis G, Yi F, Lotti JS, Layeux MS, Schultz EP, et al. Discovery of (*r*)-2-amino-3-triazolpropanoic acid derivatives as NMDA receptor glycine site agonists with GluN2 subunit-specific activity. *Front Chem* 2022;**10**:1008233.
81. Zhao F, Rouzbeh N, Hansen KB, Clausen RP. Improved synthetic route for the GluN2-specific NMDA receptor glycine site agonist AICP. *Tetrahedron Lett* 2020;**61**:151653-1-4.
82. Bettini E, Sava A, Griffante C, Carignani C, Buson A, Capelli AM, et al. Identification and characterization of novel nmda receptor antagonists selective for GluN2A over GluN2B-containing receptors. *J Pharmacol Exp Therapeut* 2010;**335**:636−44.
83. Yi F, Mou TC, Dorsett KN, Volkmann RA, Menniti FS, Sprang SR, et al. Structural basis for negative allosteric modulation of GluN2A-containing NMDA receptors. *Neuron* 2016;**91**:1316−29.
84. Hansen KB, Ogden KK, Traynelis SF. Subunit-selective allosteric inhibition of glycine binding to NMDA receptors. *J Neurosci* 2012;**32**:6197−208.
85. Müller SL, Schreiber JA, Schepmann D, Strutz-Seebohm N, Seebohm G, Wünsch B. Systematic variation of the benzenesulfonamide part of the GluN2A selective NMDA receptor antagonist Tcn-201. *Eur J Med Chem* 2017;**129**:124−34.
86. Rajan R, Schepmann D, Schreiber JA, Seebohm G, Wünsch B. Synthesis of GluN2A-selective NMDA receptor antagonists with an electron-rich aromatic b-ring. *Eur J Med Chem* 2021;**209**:112939.
87. Rajan R, Schepmann D, Steigerwald R, Schreiber JA, El-Awaad E, Jose J, et al. [2.2]Paracyclophane-based Tcn-201 analogs as GluN2A-selective NMDA receptor antagonists. *ChemMedChem* 2021;**16**:3201−9.
88. Steigerwald R, Chou TH, Furukawa H, Wünsch B. GluN2A-selective NMDA receptor antagonists: mimicking the U-shaped bioactive conformation of Tcn-201 by a [2.2]paracyclophane system. *ChemMedChem* 2022;**17**:e202200484.
89. Schreiber JA, Müller SL, Westphälinger SE, Schepmann D, Strutz-Seebohm N, Seebohm G, et al. Systematic variation of the benzoylhydrazine moiety of the GluN2A selective nmda receptor antagonist Tcn-201. *Eur J Med Chem* 2018;**158**:259−69.
90. Volkmann RA, Fanger CM, Anderson DR, Sirivolu VR, Paschetto K, Gordon E, et al. Mpx-004 and Mpx-007: new pharmacological tools to study the physiology of nmda receptors containing the GluN2A subunit. *PLoS One* 2016;**11**:e0148129.
91. Monaghan DT, Irvine MW, Costa BM, Fang G, Jane DE. Pharmacological modulation of nmda receptor activity and the advent of negative and positive allosteric modulators. *Neurochem Int* 2012;**61**:581−92.
92. Xiang Z, Conn PJ. Novel pams targeting NMDAR GluN2A subunit. *Neuron* 2016;**89**:884−6.
93. Volgraf M, Sellers BD, Jiang Y, Wu G, Ly CQ, Villemure E, et al. Discovery of GluN2A-selective NMDA receptor positive allosteric modulators (pams): tuning deactivation kinetics *via* structure-based design. *J Med Chem* 2016;**59**:2760−79.
94. Hackos DH, Lupardus PJ, Grand T, Chen Y, Wang TM, Reynen P, et al. Positive allosteric modulators of GluN2A-containing NMDARs with distinct modes of action and impacts on circuit function. *Neuron* 2016;**89**:983−99.
95. Goldsmith PJ. NMDAR pams: multiple chemotypes for multiple binding sites. *Curr Top Med Chem* 2019;**19**:2239−53.
96. Trabanco AA, Bartolomé JM, Cid JM. Mglur2 positive allosteric modulators: an updated patent review (2013−2018). *Expert Opin Ther Pat* 2019;**29**:497−507.
97. Musazzi L. Targeting metabotropic glutamate receptors for rapid-acting antidepressant drug discovery. *Expet Opin Drug Discov* 2021;**16**:147−57.
98. Geoffroy C, Paoletti P, Mony L. Positive allosteric modulation of NMDA receptors: mechanisms, physiological impact and therapeutic potential. *J Physiol* 2022;**600**:233−59.
99. Zhan P, Itoh Y, Suzuki T, Liu X. Strategies for the discovery of target-specific or isoform-selective modulators. *J Med Chem* 2015;**58**:7611−33.
100. Hackos DH, Hanson JE. Diverse modes of NMDA receptor positive allosteric modulation: mechanisms and consequences. *Neuropharmacology* 2017;**112**:34−45.
101. Wang TM, Brown BM, Deng L, Sellers BD, Lupardus PJ, Wallweber HJA, et al. A novel NMDA receptor positive allosteric modulator that acts *via* the transmembrane domain. *Neuropharmacology* 2017;**121**:204−18.
102. Hanson JE, Ma K, Elstrott J, Weber M, Saillet S, Khan AS, et al. GluN2A NMDA receptor enhancement improves brain oscillations, synchrony, and cognitive functions in Dravet syndrome and Alzheimer's disease models. *Cell Rep* 2020;**30**:381−96.
103. Villemure E, Volgraf M, Jiang Y, Wu G, Ly CQ, Yuen PW, et al. GluN2A-selective pyridopyrimidinone series of NMDAR positive allosteric modulators with an improved *in vivo* profile. *ACS Med Chem Lett* 2017;**8**:84−9.
104. Sakurai F, Yukawa T, Kina A, Murakami M, Takami K, Morimoto S, et al. Discovery of pyrazolo [1,5-*a*] pyrazin-4-ones as potent and brain penetrant GluN2A-selective positive allosteric modulators reducing AMPA receptor binding activity. *Bioorg Med Chem* 2022;**56**:116576.
105. Coaviche-Yoval A, Trujillo-Ferrara JG, Soriano-Ursúa MA, Andrade-Jorge E, Sánchez-Labastida LA, Luna H, et al. *In silico* and *in vivo* neuropharmacological evaluation of two γ-amino acid isomers derived from 2,3-disubstituted benzofurans, as

ligands of GluN1-GluN2A NMDA receptor. *Amino Acids* 2022;**54**:215−28.
106. Li Z, Cai G, Fang F, Li W, Fan M, Lian J, et al. Discovery of novel and potent *N*-methyl-D-aspartate receptor positive allosteric modulators with antidepressant-like activity in rodent models. *J Med Chem* 2021;**64**:5551−76.
107. Wang YT, Peter AC. *N*-Methyl-D-aspartate receptor allosteric modulators and methods for their use. 2021. US patent 11,166,924, 2021-11-9.
108. Romero-Hernandez A, Furukawa H. Novel mode of antagonist binding in NMDA receptors revealed by the crystal structure of the GluN1-GluN2A ligand-binding domain complexed to NVP-AAM077. *Mol Pharmacol* 2017;**92**:22−9.
109. Lind GE, Mou TC, Tamborini L, Pomper MG, De Micheli C, Conti P, et al. Structural basis of subunit selectivity for competitive NMDA receptor antagonists with preference for GluN2A over GluN2B subunits. *Proc Natl Acad Sci U S A* 2017;**114**:6942−51.
110. Jespersen A, Tajima N, Fernandez-Cuervo G, Garnier-Amblard EC, Furukawa H. Structural insights into competitive antagonism in NMDA receptors. *Neuron* 2014;**81**:366−78.
111. Conti P, Pinto A, Tamborini L, Madsen U, Nielsen B, Bräuner-Osborne H, et al. Novel 3-carboxy- and 3-phosphonopyrazoline amino acids as potent and selective NMDA receptor antagonists: design, synthesis, and pharmacological characterization. *ChemMedChem* 2010;**5**:1465−75.
112. Tamborini L, Chen Y, Foss CA, Pinto A, Horti AG, Traynelis SF, et al. Development of radiolabeled ligands targeting the glutamate binding site of the *N*-methyl-D-aspartate receptor as potential imaging agents for brain. *J Med Chem* 2016;**59**:11110−9.
113. Lai Y, Chu X, Di L, Gao W, Guo Y, Liu X, et al. Recent advances in the translation of drug metabolism and pharmacokinetics science for drug discovery and development. *Acta Pharm Sin B* 2022;**12**:2751−77.
114. Wu C, Liu Y, Yang Y, Zhang P, Zhong W, Wang Y, et al. Analysis of therapeutic targets for SARS-CoV-2 and discovery of potential drugs by computational methods. *Acta Pharm Sin B* 2020;**10**:766−88.